Journal of Medicinal Chemistry

Article

Adventures in Scaffold Morphing: Discovery of Fused Ring Heterocyclic Checkpoint Kinase 1 (CHK1) Inhibitors

Bin Yang, Melissa Vasbinder, Alexander W. Hird, Qibin Su, Haixia Wang, Yan Yu, Dorin Toader, Paul D Lyne, Jon A. Read, Jason Breed, Stephanos Ioannidis, Chun Deng, Michael Grondine, Nancy DeGrace, David Whitston, Patrick Brassil, and James W Janetka

J. Med. Chem., **Just Accepted Manuscript** • Publication Date (Web): 04 Jan 2018

ACS Publications

Journal of Medicinal Chemistry is published by the American Chemical Society. 1155 Sixteenth Street N.W., Washington, DC 20036

Adventures in Scaffold Morphing: Discovery of Fused Ring Heterocyclic Checkpoint Kinase 1 (CHK1) Inhibitors

Bin Yang[1]*, Melissa M. Vasbinder, Alexander W. Hird[1], Qibin Su[1], Haixia Wang[1], Yan Yu, Dorin Toader[∞], Paul D. Lyne[1], Jon A. Read[2], Jason Breed[2], Stephanos Ioannidis, Chun Deng[×], Michael Grondine[1], Nancy DeGrace, David Whitston[1], Patrick Brassil[¶] and James W. Janetka[⊥]

[1]*Oncology Chemistry, IMED Biotech Unit, AstraZeneca, 35 Gatehouse Drive, Waltham MA 02451, USA*

[2]*Discovery Sciences, IMED Biotech Unit, AstraZeneca, Building 310, Cambridge Science Park, Milton Road, Cambridge UK*

ABSTRACT

Checkpoint kinase-1 (CHK1) inhibitors are potential cancer therapeutics which can be utilized for enhancing the efficacy of DNA damaging agents. Multiple small molecule CHK1 inhibitors from different chemical scaffolds have been developed and evaluated in clinical trials in combination with chemotherapeutics and radiation treatment. Scaffold morphing of thiophene carboxamide ureas (TCUs), such as AZD7762 (**1**) and a related series of triazoloquinolines (TZQs), led to the identification of fused-ring bicyclic CHK1 inhibitors, 7-carboxamide thienopyridines (7-CTPs) and 7-carboxamide indoles. X-ray crystal structures reveal a key intramolecular non-covalent sulfur-oxygen interaction in aligning the hinge-binding carboxamide group to the thienopyridine core in a coplanar fashion. An intramolecular hydrogen bond to an indole NH, was also effective in locking the carboxamide in the preferred bound conformation to CHK1. Optimization on the 7-CTP series resulted in the identification of lead compound **44**, which displayed respectable drug-like properties and good *in vitro* and *in vivo* potency.

INTRODUCTION

Both normal and tumor cells employ strictly regulated DNA damage repair (DDR) pathways to survive DNA damage induced by ultraviolet rays, chemical, or replication errors, or chemotherapeutic and radiation treatments for cancer patients. It is well established that disruption of DNA repair pathways is a promising therapeutic strategy that can be used to sensitize the effects of DNA-damaging treatments.[1] An attractive approach to modulating DNA repair activity and thus potentially improving the therapeutic index of DNA-damaging therapy is to interfere with cell cycle checkpoint signaling. Checkpoint kinase-1 (CHK1, CHEK1) and checkpoint kinase-2 (CHK2, CHEK2) are Ser/Thr protein kinases that mediate the cellular response to DNA-damage. In response to DNA-damage, CHK1 is activated by phosphorylation of residues Ser-317 and/or Ser-345 by ATR kinase, and tumor cells subsequently undergo S or G2/M phase cell-cycle arrest, primarily driven by CDK inhibition, allowing cells to repair damaged DNA.[2] CHK2 is activated by phosphorylation on Thr-68 mediated by ATM kinase in response to DNA damage and causes cell cycle arrest at the G1 phase. A CHK1 inhibitor would allow a cell with damaged DNA to abrogate the cell cycle arrest and progress through the cell-cycle, ultimately leading to mitotic catastrophe and/or apoptosis.[3,4] CHK1 inhibitors have attracted substantial interest from both academia and industry as potential cancer therapeutics, and a number of diverse CHK1 inhibitors have been disclosed and evaluated in human clinical trials.[5-12] We previously reported two series of structurally distinct CHK1 inhibitors, thiophene carboxamide ureas (TCUs) and triazoloquinolones (TZQs) (**Figure 1**). Our past efforts identified the clinical candidate **1** (AZD7762), a small molecule agent that could be dosed intravenously in combination with standard chemo- or radiotherapies and

selectively sensitize p53-negative tumors over normal cells.[13-15] Herein, we report on our expanded medicinal chemistry exploration of CHK1 inhibitors and discovery of two new series of thienopyridine and indole carboxamide bicyclic CHK1 inhibitors, derived from X-ray structure-based modification or 'scaffold morphing' of the TCU and TZQ chemical series. Notably we first disclosed this work in an earlier patent publication[16] which was subsequently followed by a report of similar compounds from others.[18]

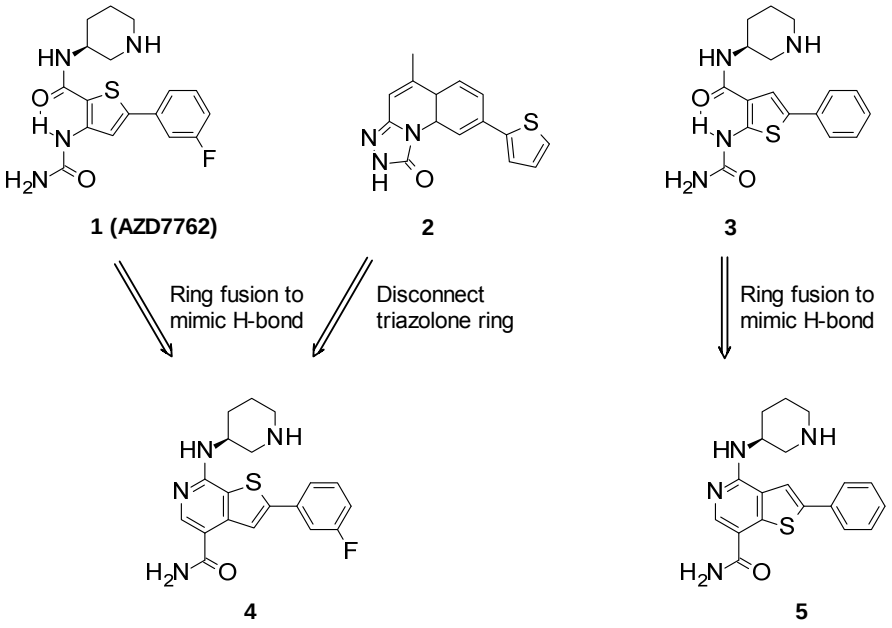

Figure 1. TCU and triazoloquinolone CHK1 inhibitors and their fused ring analogs using a scaffold morphing strategy.

RESULTS AND DISCUSSION

We previously reported X-ray crystallography data on our CHK1 inhibitors in which we elucidated that the urea carbonyl group in the TCU and the triazolone carbonyl in the TZQ compounds form the key hinge-binding interaction with the backbone NH of Cys-87 in the ATP-binding pocket of CHK1 (PDB code 2YDK[14] and 2X8E[15]). Furthermore, the urea NH forms an H-bond to the backbone carbonyl of Glu-85, in addition to three

polar interactions between the protonated piperidine nitrogen and the CHK1 residues, Asp-148, Glu-134, and Asn-135, at the edge of the ribose binding pocket (**Figure 2**).[14] We made a key observation that compound **1** and its matched pair isomeric thiophene, **3** both adopt a bound conformation having an intramolecular H-bond between the internal urea NH to the C-2 (**1**) or C-3 carbonyl (**3**) of the amide group (blue dotted line in **Figure 1**). Thus, we envisioned that a 5,6-bicyclic ring system, such as the thienopyridine core in **4** and **5** (**Figure 1**), would mimic this intramolecular hydrogen bond existing in the TCU inhibitors. Separately, disconnecting the hydrazide bond of the 5-membered triazolone ring in the TZQ scaffold also generates a similar bicyclic core that the thienopyridine group resembles. Guided by the above structural insight from two distinct chemotypes, we undertook a 'scaffold morphing' strategy to explore the potential for a variety of 5,6-bicyclic scaffolds as novel CHK1 inhibitors.

Scaffold morphing of TCU to 4-CTPs and 7-CTPs.

Due to its closest similarity to the clinical candidate TCU **1**, we first pursued the synthesis and evaluation of thienopyridine **4** and the des-fluoro analog **12**. Shown in **Scheme 1**, the synthesis of **4** starts with a Knoevenagel type condensation of glyoxylic acid with 2-(3-thienyl)acetonitrile to afford the unsaturated carboxylate **7**. Subsequently the acid was transformed to the acyl chloride followed by reaction with sodium azide to give acyl azide **8** in overall 82% yield. Curtius rearrangement of the acyl azide followed by electrophilic cyclization onto the thiophene ring at high temperatures yielded the fused ring thienopyridone **9**. The 2-position of the thiophene ring was selectively brominated with *N*-bromosuccinimide followed by treatment with phosphorus oxychloride to give chloropyridine intermediate **10**, which was further displaced by 1-*N*-Boc-protected (*S*)-3-aminopiperidine in the presence of potassium

carbonate in NMP. The resultant bromo-thienopyridine **11** was coupled to *m*-fluoro-phenylboronic acid using a palladium-catalyzed Suzuki reaction. The desired thienopyridine carboxamide **4** was generated by partial hydrolysis of the nitrile to the carboxamide with simultaneous Boc deprotection using polyphosphoric acid. We labeled this scaffold 4-CTP since the carboxamide group is substituted on C-4 of the thienopyridine core. Compound **12** was generated in a similar fashion to **4** from **11** using phenylboronic acid.

Scheme 1. Synthesis of 4-CTP **4.**[a]

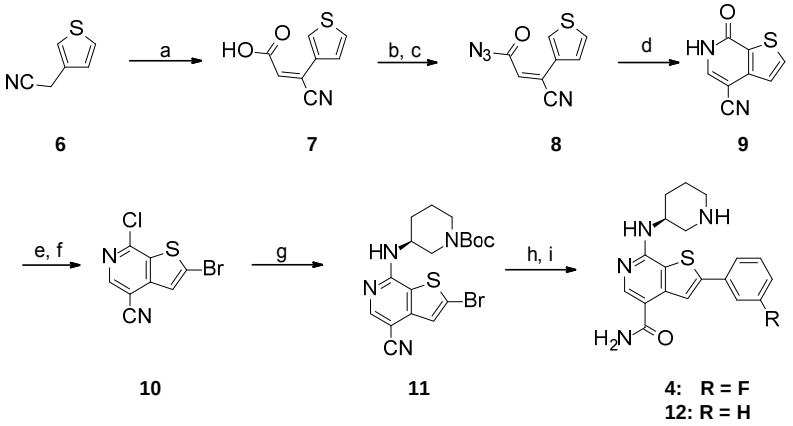

[a]Reagents and conditions: (a) glyoxylic acid, K_2CO_3, MeOH, reflux, 3h, 90% yield; (b) oxalyl chloride, DCM, rt, 63% yield; (c) NaN_3, dioxane/water, rt, 1.5 h, 82% yield; (d) diphenyl ether, 230 °C, 0.5 h, 44% yield; (e) NBS, AcOH/DMF, 80 °C, 1 h, 96% yield; (f) $POCl_3$, 110 °C, overnight, 82% yield; (g) (*S*)-3-amino-Boc-piperidine, K_2CO_3, NMP, 80 °C, quantitative yield; (h) $Pd(Ph_3P)_4$, *m*-F-PhB$(OH)_2$, Cs_2CO_3, dioxane/water, 80 °C, 54% yield; (i) PPA, 110 °C, 12 h.

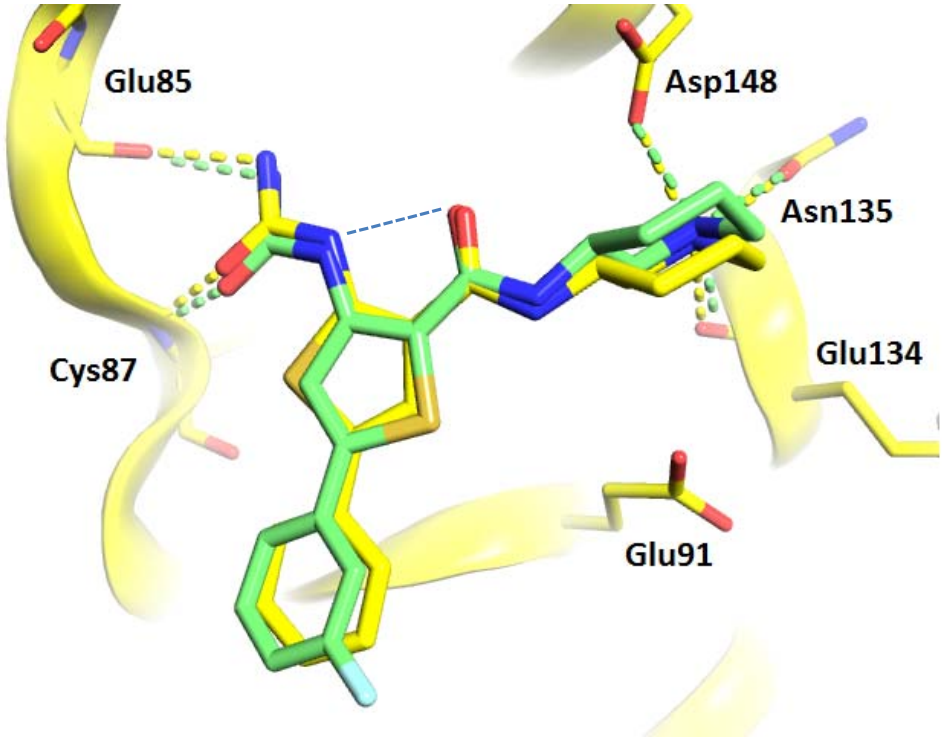

Figure 2. X-ray crystal structure overlay of compounds **1** and **3** bound to human CHK1 kinase domain. Carbon atoms and hydrogen bonds of **1** bound to CHK1 are colored green and carbon atoms of **3** are colored yellow (PDB codes 2YDJ and 2YDK respectively. Selected residues and inhibitors are depicted as sticks. Picture was generated in PYMOL).

Surprisingly, both compounds **4** and **12** showed very weak potency (500-1000 fold drop vs. **1**) in the CHK1 biochemical assay (**Table 1**). We suspected that the steric repulsion between the carbonyl group of the C-4 carboxamide and C-3 hydrogen forced the carboxamide out of the plane of the thienopyridine bicycle, rendering the binding conformation of compounds **4** and **12** to CHK1 protein a high energy state. In **Figure 2**, the urea groups in both compounds **1** and **3** share a coplanar conformation with the thiophene ring, which likely contributes to their potent activity in CHK1 inhibition. A search of similar analogs in our internal crystal structure database

revealed that in similar ligands with primary carboxamide groups substituted at C-4 of the 5,6-bicyclic heteroaryl core, the dihedral angle was measured to be 25-30 degrees, significantly larger than we measured in both TCUs (15.1° for **1** and 15° for **3**). Despite their weaker potency, we demonstrated that 4-CTPs **4** and **12** had improved properties relative to TCU **1**, including weaker hERG inhibition (**Table 1**).

Table 1. CHK1 potency and hERG IC_{50}s of **1** and its 4-CTP analogs.

Compound	CHK1 IC_{50} (μM)[*a]	hERG IC_{50} (μM)
1	0.005	15
4	6.8	>31.6
12	2.6	>31.6

[*]IC_{50} represents activity of the compound in a CHK1 biochemical assay.

[a]IC_{50} values are the geometric mean of at least two measurements.

We surmised that an alternative thienopyridine analog would be a direct mimic to compound **3**, essentially flipping the sulfur in 4-CTP to the carboxamide side of the thienopyridine core to give compound **5**. In this 7-carboxamide-thienopyridine (7-CTP) scaffold, the close proximity of the carboxamide carbonyl group and the sulfur atom in the thiophene ring would make the non-covalent oxygen-sulfur interaction possible, and we hypothesized that it would enable the 7-CTP compounds to adopt a conformation that better mimics the coplanar feature between the carboxamide group and thiophene ring in **1** and **3**. Therefore, we synthesized 7-CTP analogs using a similar route to the syntheses of compounds **4** and **12**, starting from commercially

available 2-(2-thienyl)acetonitrile. CHK1 potency, aqueous solubility, and hERG inhibition of these compounds are shown in **Table 2**. To our delight, the 7-CTP compounds indeed showed excellent activity in CHK1 inhibition. Inhibitors **5** and **13** are matched pairs of **12** and **4**, yet their IC_{50}s are vastly improved and reach the same levels of potency as the original TCU compounds **1** and **3**. Based on TZQ analog **2**, two analogs containing thiophene substituents incorporated at the 2-position, were also synthesized, also showing similar potency to **5**. Encouraged by these promising results, the 7-CTP inhibitors were tested in our previously described HT29 cell abrogation assay.[13] Compounds **5**, **13**, **14**, and **15** indeed proved to be extremely potent in abrogating the HT29 cell-cycle arrest caused by camptothecin-induced DNA damage. Further profiling of these compounds revealed they have good aqueous solubility and moderate to low activity in hERG inhibition (**Table 2**). However, when tested for their *in vivo* pharmacokinetic properties, these compounds were found to have very high systemic clearance in the rat (exceeding rat liver blood flow),

warranting a further optimization effort to increase their half-life and improve their *in vivo* exposure.

Table 2. Potency and properties of close analogs of **4** and **12** with 7-CTP core.

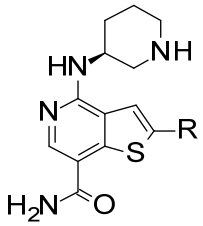

	R	CHK1 IC_{50} (μM)[α]	Abrogation EC_{50} (μM)[ab]	Solubility (μM)[c]	hERG IC_{50} (μM)	Rat clearance CL (ml/min/kg)
3		0.007	0.019	>2000	>31.6	49
5	Ph	0.007	0.026	>1000	19.7	>72
13	m-F-Ph	0.012	0.024	334	14.2	>72
14	2-thienyl	0.015	0.012	>1000	>30	>72
15	3-thienyl	0.006	0.010	980	28	>72

[a]IC_{50} and EC_{50} values are the geometric mean of at least two measurements.

[b]EC_{50} represents cellular activity in cells pretreated with a DNA-damaging agent, camptothecin, prior to compound treatment. [b]Solubility is measured using solids from evaporated DMSO solution.

In our previous communications on TZQ CHK1 inhibitors, pyrazoles which occupy the solvent channel of CHK1, in place of the thiophene group in compound **2** were tolerated.[15] Using this as precedent, we grafted those more hydrophilic heterocycles to the new 7-CTP scaffold, installing them on C-2 of the 7-CTP core (**Table 3**), to reduce the lipophilicity of 7-CTPs as a strategy to address metabolic stability issues and to improve margin over hERG inhibition. Nevertheless, while we found CHK1 enzyme potency was retained with these heteroaryl substituents, pyrazoles, **16** and

17, and imidazole, **19**, caused a drop in cell potency, likely due to reduced cell permeability, as lower cLogP (**16** and **19** compared with **18**) or an additional hydrogen bond donor (**16** compared with **17**) is associated with larger biochemical to cellular potency drop-off. Benzyl pyrazole **18** maintained cellular potency, but had high lipophilicity (cLogP = 4.0) due to the hydrophobic benzyl substitution. We also evaluated analogs with smaller C-2 substituents such as methyl group at C-2 (**20**) but found significantly reduced CHK1 potency, suggesting an aromatic ring or larger groups at C-2 is essential.

Table 3. Heteroaryl or alkyl substitutions at C-2 of 7-CTP reduced CHK1 cellular potency.

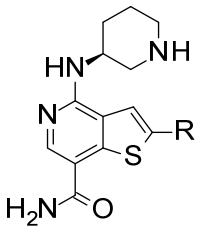

	R	CHK1 IC_{50} (μM)[a]	Abrogation EC_{50} (μM)[a]	CLogP
16	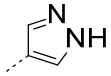	0.020	2.3	2.0
17	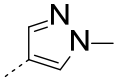	0.006	0.15	2.0
18	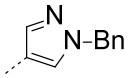	0.014	0.06	4.0
19		0.024	10	1.7
20	Me	0.15	ND*	2.3

[a]IC_{50} and EC_{50} values are the geometric mean of at least two measurements

* Not determined.

Modification of thienopyridines to indoles

Intramolecular sulfur-oxygen interactions are known to be isosteric to hydrogen-bonding interactions.[17] Recognizing the carbonyl oxygen and thiophene sulfur interaction in 7-CTPs was critical for the potency of the already explored bicyclic scaffolds, we were intrigued by the potential of an indole core that can offer an intramolecular hydrogen bond between the carbonyl of the carboxamide group and the indole NH (**Figure 3**). We surmised that a hydrogen bond can lock the 7-carboxamide of the indole compound **21** in the desired conformation for its optimal binding to CHK1.

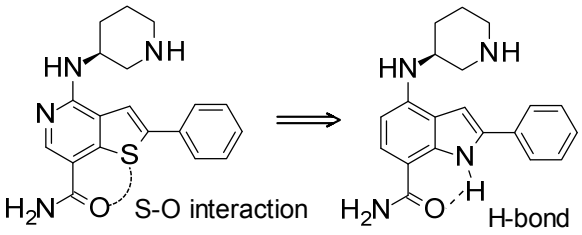

5 **21**

Figure 3. Isosteric replacement of S-O interaction using the hydrogen bond of the indole NH.

Illustrated in **Scheme 2** is the synthetic route to the initially designed indole analog **21**, based on 7-CTP **5**. The nitro anthranilate derivative **22** was converted to methyl ester **23** using thionyl chloride in methanol under reflux conditions. Ester **23** then underwent a novel one-pot multi-step transformation using potassium *tert*-butoxide in DMSO which involved generation of an enamine by reaction with acetophenone and nucleophilic aromatic substitution *ortho* to the activating nitro group, followed by air oxidation to produce the indole carboxylic acid **24**. The indole intermediate **24** was

converted to amide **25** upon treatment of isobutyl chloroformate and ammonia. Hydrogenation of the nitro group of **25** yielded the aniline compound **26**, which was then converted to the anticipated racemic version of the product **21** by reductive amination with Boc protected 3-oxopiperidine in good yield. Chiral separation of the racemic mixture of **21** by chrial preparative HPLC afforded the desired *S*-enantiomer **21** and its *R*-enantiomer (*R*)-**21**.

Scheme 2. Synthesis of indole analog **21**.[b]

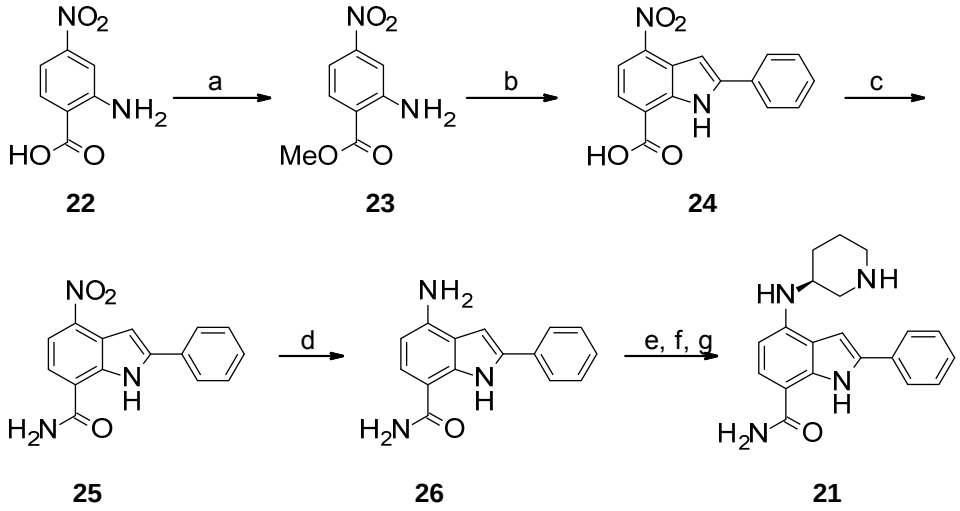

[b]Reagents and conditions: (a) $SOCl_2$, MeOH, reflux, 2 days, 63% yield; (b) acetophenone, KO*t*-Bu, DMSO, -15 °C, 1 h, 90%; (c) isobutyl chloroformate, NH_3, DCM, -15 °C to rt, 80% yield; (d) H_2, 10% Pd/C, rt, overnight, MeOH, 80% yield; (e) 3-oxo-Boc-piperidine, Na_2SO_4, $NaBH(OAc)_3$, rt, AcOH, 30% yield; (f) 4N HCl in dioxane, MeOH, 2 h, 78% yield; (g) chiral preparative HPLC for enantiomeric separation.

In addition to **21**, three additional analogs bearing *m*-fluorophenyl, *p*-fluorophenyl, and *p*-chlorophenyl groups at C-2 of the indole core were also synthesized (**27**, **28**, and **29, Table 4**). As we expected, these indole analogs proved to be equal or slightly less

potent relative to their matched pairs of **5** and **13**, both in the CHK1 inhibition assay and in the cell-cycle abrogation assay. The aqueous solubility of compound **21** is still respectable at 280 μM but lower than the matched 7-CTP analog **5**. An unanticipated concern for these indole compounds, however, is their hERG inhibition liability, as shown in **Table 4**. All four analogs (**21** and **27**-**29**) are more potent hERG inhibitors compared with their 7-CTP matched pairs. Compound **21**, as a representative from this sub-series of CHK1 inhibitors, was taken into rat *in vivo* PK studies, and similar to its 7-CTP analog, **(*S*)-1** showed high clearance (CL: 160 mL/min/mg), high volume of distribution (Vss: 46 L/kg), and a short half-life ($t_{1/2}$: 2.6 h).

To further test the importance of the non-covalent intramolecular interaction perceived to exist both in 7-CTPs and in the indole analogs (**21** and **27**-**29**), we synthesized a furopyridine compound **30**, aiming to deprive the hydrogen bond interaction between the NH and the carboxamide carbonyl group of indole **21**. As we expected, switching indole NH in **21** to O in **30** caused a 10-fold drop in potency, confirming the critical role of the intramolecular electrical interaction for these CHK1 inhibitors, existing in 7-CTPs as an oxygen-sulfur interaction and in the indoles as a hydrogen bond. Consistent with our observations first reported in 2006[16] and now a complete account herein, a series of CHK1 inhibitors published by Zhao et. al. also contains additional 5,6-bicyclic aromatic cores, such as thiazolopyridine and thiazolopyridazine, which embed the sulfur atom next to the carboxamide group.[18] Presumably, the oxygen-sulfur interaction also strongly contributed to the potency in a similar fashion to that seen in these 7-CTP examples.

Next, we obtained X-ray crystal structures for both compounds **13** and **21** bound to

CHK1. Undeniably, these two molecules superimposed on each other and TCUs **1** and **3** closely, both maintaining a near coplanar conformation between the carboxamide group and the bicyclic heteroaryl core, and made analogous polar and non-polar interactions with the CHK1 protein (**Figure 4**). Same as in both TCUs (**1** and **3**, **Figure 1**), the carboxamides of **13** and **21** make hydrogen-bonding interactions with the hinge residues Glu-85 and Cys-87. Their protonated piperidine nitrogens make three polar interactions in the ribose binding pocket, including to Asp-148, Glu-134, and Asn-135. In both structures, the C-4 NH interacts with the terminal carboxylate of Glu-91 through a water molecule. The indole or thienopyridine bicyclic core is sandwiched between the hydrophobic side chains of Val-23 and Leu-15 of the P-loop and Leu-137 of the catalytic loop (not shown in **Figure 4**). The indole NH of **21** makes no direct polar interactions with CHK1, unlikely to directly contribute to the binding affinity of **21** to CHK1 other than the intramolecular hydrogen-bonding to the carboxamide group. Here, we experimentally demonstrated that the indole NH was an effective isosteric replacement to the sulfur atom in 7-CTPs and good potency was achieved with the indole core. However, due to the concern on the hERG activity of these indole compounds, we shifted our focus back to the thienopyridines.

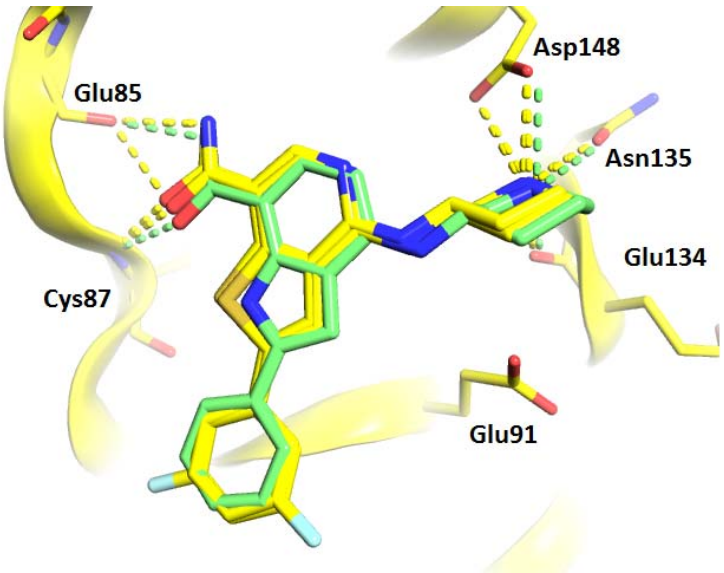

Figure 4. X-ray crystal structure overlay of compounds **13** and **21** bound to human CHK1 kinase domain. Carbon atoms and hydrogen bonds of **13** bound to CHK1 are colored yellow and carbon atoms of **21** are colored green (PDB codes are 6FC8 for **13** and 6FCK for **21**). **13** is modelled as a dual conformation. Selected residues and inhibitors are depicted as sticks. Picture was generated in PYMOL).

Table 4. CHK1 potency, solubility, and hERG inhibition of indole and furopyridine analogs.

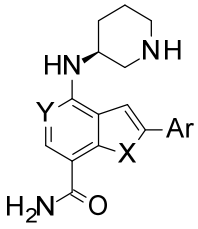

	Ar	X	Y	CHK1 IC_{50} (μM)[a]	Abrogation EC_{50} (μM)[a]	Solubility (μM)	hERG IC_{50} (μM)
21	Ph	NH	CH	0.031	0.053	280	11.6
27	*m*-F-Ph	NH	CH	0.009	0.030	ND[b]	7.7
28	*p*-F-Ph	NH	CH	0.023	0.040	380	6.7
29	*p*-Cl-Ph	NH	CH	0.015	0.070	320	4.1
30[c]	Ph	O	N	0.33	0.39	>1000	ND[b]

[a]IC_{50} and EC_{50} values are the geometric mean of at least two measurements

[b]Not determined.

[c]For the synthesis of the furopyridine analog **30**, see Supporting Information.

Optimization of the amino-piperidine group

Our previous work on TCUs explored the SAR of the solvent channel aryl groups (equivalent to the C-2 aryl on 7-CTPs) extensively, and simple phenyl or halogen

substituted phenyl groups were identified to offer a better overall profile.[13] As previously noted, we and others also published extensive C-2 aryl or heteroaryl SAR exploration on the thienopyridine core as CHK1 inhibitors.[17] As summarized in **Table 2** and **Table 4**, neither the variation on the C-2 aryl groups of the 7-CTP core nor switching the core from CTP to indole effectively lowered the *in vivo* rat clearance. Shown in **Table 5** is the measured intrinsic clearance when compounds (**5**, **14**, **15**, and **21**) were incubated with human or rat liver microsomes. Consistent with the observed high *in vivo* rat clearance, these compounds showed moderate to high CLint in rat microsomal studies, although their human microsomal CLints were more moderate. Our earlier SAR studies on the TCUs identified 3-(*S*)-aminopiperidine as a more potent group,[13,14] and we suspected the high rat clearance for both the thienopyridine and indole compounds at least was partially due to the metabolic liability of the amino-piperidine group. Herein, we set out to further study the SAR around the aminopiperidine group in 7-CTPs to address metabolic stability and hERG issues associated with this series of compounds.

While it was not clear to us if the C-4 NH played a role in contributing to the metabolic instability of the 7-CTPs, we were also intrigued to know how significant its water molecule-bridged polar interaction with Glu-91 was to the potency. This interaction can be disrupted by small alkyls substitutions on the C-4 nitrogen. A list of compounds that were evaluated from this effort are shown in **Table 6**. The syntheses of these analogs followed a route very similar to that of compound **5**. Analogs **31** and **32** with the C-4 oxygen and sulfur replacements for nitrogen, respectively, were synthesized when 3-(*S*)-hydroxy or 3-sulfanyl Boc piperidine was used in step g, **Scheme 1**, but using 7-CTP as the intermediate (Supporting Information). Analogs with alkyl

substitutions on the C-4 nitrogen were obtained when *N*-substituted-Boc-piperidines were used.

When tested for CHK1 activity, both **31** and **32** showed about a 10-fold drop in potency compared with **5** in the CHK1 biochemical assay, and their cellular potency decrease was similar or more significant. Small alkyl substituents at the C-4 nitrogen of 7-CTP (compounds **33** and **34**) were slightly better in maintaining biochemical activity (3-5 fold drop), but cellular potency also dropped significantly. More polar substitutions, such as compound **35**, that contain a terminal hydroxy group on the alkyl group, brought a similar drop in biochemical activity, but their toll on cellular activity was more profound. Large hydrophobic substitution (**36**) were detrimental to potency. Interestingly, the N-methyl compound (**33**) showed improved stability in both human and rat microsomal assays, but C-4 O-linker analog **31** showed significantly reduced microsomal stability (**Table 5**). Unfortunately, these compounds, except the hydroxyethyl analog **35**, also showed increased hERG liability, and their increased lipophilicity (cLogP 3.87 for **5** and up to 4.60 for **34**) likely contributed to their promiscuous hERG inhibition.

Table 5. *In vitro* metabolic stability of 7-CTPs and indole **21**

	Core	Hu mics CLint (μL/min/mg)	Rat mics CLint (μL/min/mg)
5	7-CTP	9.2	32
14	7-CTP	9.1	36
15	7-CTP	29	72
21	Indole	21	120
31	7-CTP	35	>120

32	7-CTP	<5	11
33	7-CTP	10	37

Table 6. CHK1 potency of analogs after replacement of the thienopyridine C-4 nitrogen

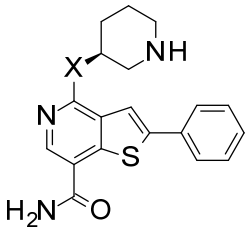

	X	CHK1 IC_{50} (μM)[a]	Abrogation EC_{50} (μM)[a]	hERG IC_{50} (μM)
31	O	0.083	0.34	3.8
32[b]	S	0.056	0.21	4.9
33	NCH_3	0.025	0.84	2.7
34	NCH_2CH_3	0.035	0.11	2.4
35	$N(CH_2)_2OH$	0.079	3.70	>31.6
36	NCH_2CH_2Ph	0.66	ND[c]	2.1

[a]IC_{50} and EC_{50} values are the geometric mean of at least two measurements

[b]racemic version only

[c]Not determined

Scheme 3. Synthesis of 3-amino-2-methyl-piperidines.[a]

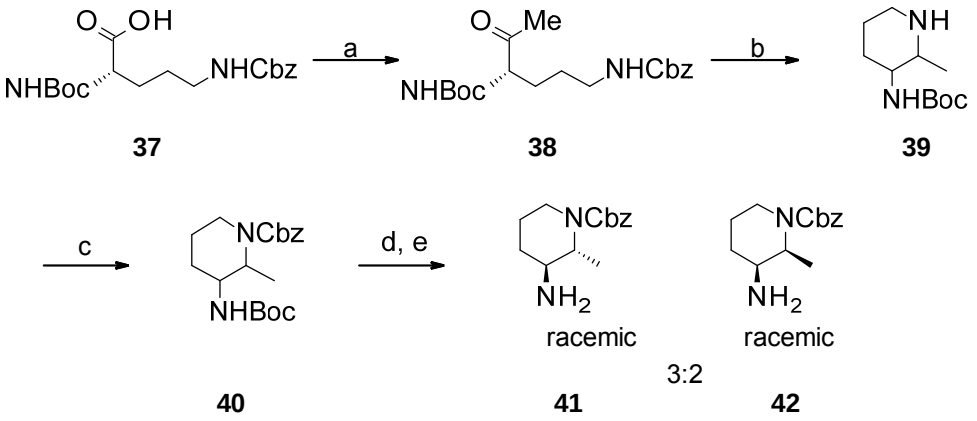

[a]Reagents and conditions: (a) MeLi, THF, 0 °C to rt, 5 h, 14% yield; (b) 10% Pd/C, H_2. MeOH, rt, 3 days, 100% yield; (c) CbzCl, DIPEA, DCM, rt, 1 h, 49% yield; (d) silica gel column separation, EtOH/hexane, 49% yield *trans* isomer and 35% yield for *cis* isomer; (e) 4N HCl in dioxane, MeOH, rt, 100% yield.

In order to address the metabolic stability concern of the 3-amino-piperidine group, we next focused on the structural modifications close to the piperidine nitrogen, as it is known that a basic nitrogen can be susceptible to oxidation by FMO (Flavin-containing monooxygenase) enzymes in the hepatocytes.[19] Reducing nitrogen pKa is a known approach in mitigating FMO induced metabolic stability, and we were also aware that the basic piperidine likely strongly contributed to the high volume of distribution of these compounds in rat PK studies.[20] However, as illustrated in the binding modes of both TCUs (**1** and **3**) and compounds **13** and **21**, the basic nitrogen was important for potency in this scaffold, so we suspected significantly modulating the pKa of the piperidine group would not be a viable strategy. We instead focused on introducing different substitutions on the piperidine ring, anticipating that these substitutions could afford more metabolically stable compounds while maintaining CHK1 potency. Shown in **Table 7** are a series of compounds that we constructed in this study.

The key for the syntheses of the piperidine-modified compounds in **Table 7** was to obtain the piperidine intermediates with a variety of substitutions and stereoisomers. Illustrated in **Scheme 3** is the route to the Cbz protected 3-amino-2-methyl-piperidine intermediate for compounds **44** and **45**. Protected L-ornithine **37** reacted directly with methyllithium to yield ketone **38** which underwent cyclization under hydrogenation conditions to form a mixture of four piperidine diastereomers **39**, due to racemization at the alpha stereocenter. The Cbz group was reinstalled to the ring nitrogen to facilitate the separation of *trans* and *cis* diastereomers, and Boc deprotection provided the Cbz protected 3-amino-piperidine intermediates, setting the stage for synthesis of the final inhibitors (c.f. steps g-l in **Scheme 1**). The *trans* racemic mixture **41** led to the desired pure enantiomer **44** after chiral HPLC separation, while the c*is* racemic mixture **42** led to **45**.

Simple methyl substitution on the ring nitrogen in piperidine (**43**) caused a 20-fold potency drop from **5**, confirming the importance of the multi-point polar interaction between the piperidine (**Figure 4**) and the CHK1 ribose binding pocket residues. Interestingly, one of the two diastereomers synthesized from 3-amino-2-methyl-piperidine intermediates, the (2*R*,3*S*)-diastereomer (**44**), showed superior potency over the other diastereomer **45**, offering similar potency to **5**. We later obtained the X-ray crystal structure for **44** (**Figure 5**). The binding mode of **44** is nearly identical to **3** and maintained all of the polar or hydrophobic interactions. As expected with **44**, the 2-methyl group *trans* to the 3-amino group on the piperidine ring adopted the equatorial conformation, directing it toward Leu-137. The presumed axial 2-methyl in **45** is less preferred. A *trans* 4-hydroxyl substituted piperidine analog (**46**) retained biochemical activity, but cellular potency dropped significantly. A more extended *trans*

2-hydroxylethyl group on the piperidine ring was not well tolerated for potency (**47**). The all *cis* tri-substituted piperidine analog **48** showed comparably good enzyme and cellular potency. The *cis*-racemic mixture of 3-amino-6-methyl-piperidine analogs were also synthesized (**49**) and it remained reasonably potent. Interestingly, the diastereomeric pair **44** and **45** showed significantly different hERG activity, and to our delight, the more potent **44** demonstrated improved hERG profile with IC_{50}s greater than 31.6 μM, the maximum tested concentration in the assay. In addition, when tested in human and rat liver microsomal stability assays, compound **44** showed a stability improvement over **5** (< 5 μL/min/mg in human microsomes and <10 μL/min/mg in rat microsomes).

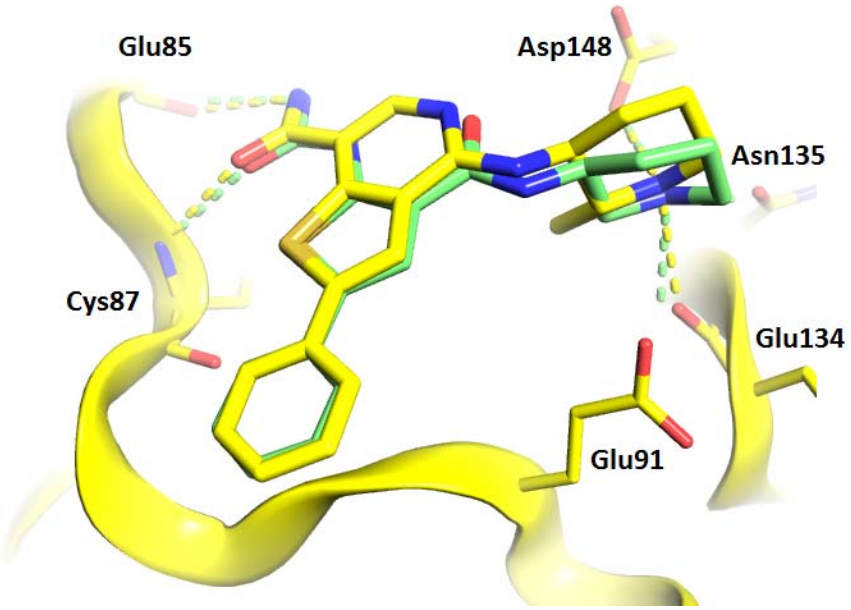

Figure 5. X-ray crystal structure overlay of compounds **44** and **3** bound to human CHK1 kinase domain. Carbon atoms and hydrogen bonds of **44** bound to CHK1 are colored yellow and carbon atoms of **3** are colored green (PDB codes are 6FCF for **44**). Selected residues and inhibitors are depicted as sticks. Pictures were generated in PYMOL.

Table 7. CHK1 potency and hERG inhibition of substituted 3-aminopiperidine analogs.

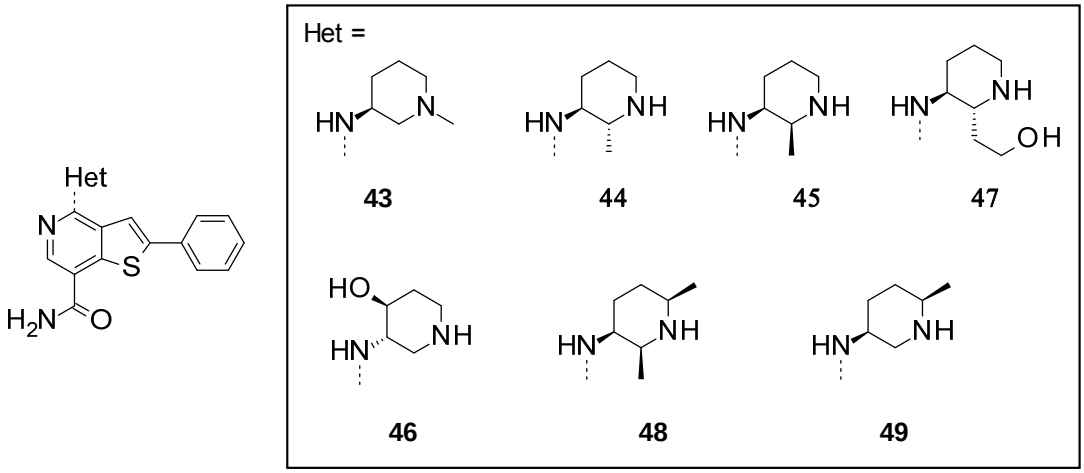

	CHK1 IC_{50} (μM)[a]	Abrogation EC_{50} (μM)[a]	hERG (μM)
43	0.14	0.88	ND[b]
44	0.006	0.008	>31.6
45	0.069	0.050	5.9
46*	0.010	0.41	>31.6
47*	0.083	3.3	>31.6
48*	0.012	0.010	8.4
49*	0.021	0.030	2.45

*racemic mixture

[a]IC_{50} and EC_{50} values are the geometric mean of at least two measurements

[b]ND: not determined

For the detailed syntheses of **43**, **46**, **47**, **48**, and **49**, see Supporting Information.

7-CTPs shows enhanced DNA-damaging effects *in vitro* and *in vivo*

To evaluate the potentiating effect of our new lead 7-CTP CHK1 inhibitors to DNA-damaging agents, such as gemcitabine, we employed a potentiation assay that was described in detail previously.[21] Briefly, the concentration-response of tumor cells to proliferation inhibition by DNA-damaging agents was measured with or without the presence of CHK1 inhibitors, which was dosed in a predefined constant concentration. The ratio of the GI_{50} from the DNA-damaging agent alone over the GI_{50} from the combination of DNA-damaging reagent and a CHK1 inhibitor was designated as the potentiation factor (PF). Compounds **5**, **13**, and **44**, along with previously reported **3**, were evaluated in this assay, each against three cell lines (SW620, MDA-MB-231, and H460-DNp53). Their potentiating effects on gemcitabine-induced cell proliferation inhibition are shown in **Table 8**. These four compounds all demonstrated synergistic effects when dosed in combination with gemcitabine. The potentiation factor (PF) was found to be more significant in the more gemcitabine-resistant cell line (H460-DNp53, an engineered cell line that was developed by retroviral infection of a dominant-negative p53 construct),[21] and less so in the more gemcitabine-sensitive cell line (MDA-MB-231). Compound **3** exhibited higher PF among these four compounds when tested in MDA-MB-231, but in the slightly less sensitive cell line SW620, all four compounds tested showed a similar level of PF. However, compound **44** stood out with a superior enhancing effect (PF = 124) when tested in H460-DNp53 cells, lowering the gemcitabine GI_{50} from 2.1 nM to 0.017 nM. The enhancing effect between **5** and **13** was marginal in both MDA-MB-231 and SW620 cells, but **13** exhibited a stronger effect in H460-DNp53 cells.

Table 8. Proliferation inhibition potentiation effect of CHK1 inhibitors when used in combination with gemcitabine.[a]

	single agent GI_{50} (nM)	single agent GI_{25} (nM)	combination GI_{50} (nM)[b]	PF[c]
MDA-MB-231				
3	596	300	0.027	9
5	536	270	0.052	5
13	641	320	0.068	4
44	306	150	0.052	5
gemcitabine	0.251			
SW620				
3	839	420	0.077	11
5	970	490	0.067	12
13	841	420	0.091	11
44	725	360	0.074	11
gemcitabine	0.84			
H460-DNp53				
3	1231	620	0.031	67
5	1798	900	0.075	28
13	2904	1450	0.055	38
44	2453	1230	0.017	124
gemcitabine	2.085			

[a]GI_{50}s and GI_{25} values are the mean value of two duplicated runs.

[b]CHK1 inhibitors concentration used in the combination with gemcitabine was its GI_{25} as a single agent.

[c]Potentiation factor

$$\frac{GI50\ (gemcitabine\ alone)}{GI50\ (gemcitabine\ in\ combination)} = PF$$

Compounds **5**, **13**, and **44** were dosed intravenously to mouse, rat, and dog to evaluate their pharmacokinetic (PK) properties (**Table 9**). All three compounds were measured to have high plasma clearance in rat, however, due to their high volume of distribution, likely resulting from the presence of the basic piperidine group, these compounds still showed reasonable half-lives. Their clearance was found to be more moderate in dog. Both in terms of CL and $t_{1/2}$, compound **5** was found to be slightly inferior in comparison to **13** and **44**. Compound **44** showed a more consistent profile across mouse and rat with lower CL, longer $t_{1/2}$, and lower Vss, and in dog its $t_{1/2}$ is notably longer, likely associated with its larger Vss in dog.

We tested these three compounds for their *in vivo* effects in a mouse Hollow Fiber (HF) model.[14,21] In this model, HCT116 cells were treated with the DNA-damaging agent topotecan to induce cell cycle arrest in the G2 phase. The hollow fibers were filled with cell cycle arrest cells and subsequently were implanted subcutaneously in mice before compounds were intravenously dosed. Implanted fibers were retrieved after 30 h to determine the cell cycle profile of the enclosed cells. When dosed with CHK1 compounds, the G2 arrest was overcome causing a reduction in the number of cells in G2 and a concomitant increase in the number of cells re-entering the G1 phase. The "odds value" was then calculated as the ratio of the G2/G1 populations for topotecan alone and the CHK1 inhibitor combination. Based on the odds value, we calculated an odds ratio (OR) that allowed quantitative assessment of the degree of checkpoint abrogation. The greater the OR, the higher the level of checkpoint abrogation. Shown in **Figure 6** are the odds ratios for **5**, **13**, and **44**. All three compounds showed G2 arrest abrogation effect in the HCT116 HF assay, with **13**

showing the lowest OR (2.0) among these three compounds. Compounds **5** and **44** demonstrated similar PD effects in this model at the same dose (10 mg/kg), with OR at 3.2 and 3.7, respectively.

Table 9. *In vivo* PK of **5**, **13**, and **44**

	5	**13**	**44**
CL (mL/min/kg) Mouse / rat / dog	45 / 295 / 11	28 / 196 / 10	29 / 105/ 10
t ½ (h) mouse / rat / dog	1.5 / 3.1 / 5.4	8.5 / 4.4 / 5.1	3.4 / 5.1/ 9.4
Vss (L/kg)* mouse / rat / dog	4.0 / 75 / 3.7	4.6 / 54.3 / 4.4	4.6 / 24 / 7.1

*Steady-state volume of distribution after intravenous dose.

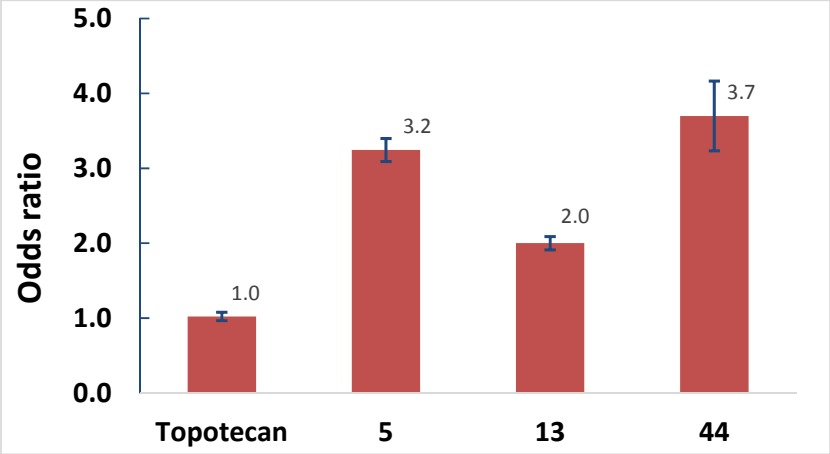

The error bars represent the standard error of the mean odds ratio of multiple runs of the study.

$$Odd = \frac{G2\%}{G1\%} \qquad Odds\ ratio = \frac{Odd\ (topotecan\ alone)}{Odd\ (treatment)}$$

Figure 6. Odds ratio of **5**, **13**, and **44** in Hollow Fiber mouse PD assay (iv administration, using HCT116 cells)

CONCLUSION

Using X-ray structure-based drug design, we employed a scaffold morphing strategy to successfully design several new series of potent CHK1 inhibitors featuring 5,6-bicyclic cores that mimic the productive conformation of TCU compounds bound to CHK1. We discovered a key intramolecular oxygen-sulfur interaction was critical for the potency of carboxamide thienopyridines (CTPs), as this interaction allows the carboxamide group to orient in a coplanar conformation with the bicyclic aromatic core. Replacement of the O-S interaction by an intramolecular hydrogen bond was proven to be effective in maintaining the critical coplanar conformation and hence resulted in similar CHK1 potency. Additional structural optimization of this class of thienopyridine compounds has led to the identification of advanced lead compound **44**, which contains a *trans* 3-amino-2-methylpiperidine group to occupy the ribose pocket of CHK1. Compound **44** encompasses a combination of excellent potency, reduced hERG liability, and improved *in vitro* metabolic stability. When used in combination with gemcitabine, it strongly enhanced the proliferation inhibition effect of gemcitabine in multiple tumor cell lines. The *in vivo* plasma clearance of **44** in rodents was found to be high, but in dog both the clearance and half-life were reasonable. When tested for its *in vivo* PD activity in combination with topotecan, compound **44** demonstrated the mode of action in abrogating HCT116 G2 cell cycle arrest induced by topotecan, which presumably would lead to eventual apoptosis of HCT116 cells. In a subsequent preclinical rat telemetry study, compound **44** was found to induce reversible hypotension and reflex tachycardia when dosed to male Han Wistar rats at 12.5 mg/kg. Given that cardiac dose-limiting toxicities occurred in patients of **1** and other CHK1 inhibitors in phase I clinical trials,[22,23] the decision was not to progress compound **44** or other CHK1 inhibitors from this class into additional preclinical and clinical studies.

Currently there are multiple CHK1 inhibitors (prexasertib, ARRY-575, and CCT-245737) (Citeline/Trialtrove, as of October, 2016) in clinical trials and it remains a hope that one or more of these inhibitors will eventually be approved, bringing important new treatment options to cancer patients.

EXPERIMENTAL SECTION

General information

All solvents used were commercially available in anhydrous grade. Reagents were utilized without further purification unless otherwise stated. Evaporation of solvent was carried out using a rotary evaporator under reduced pressure at a bath temperature of up to 60 ºC. Temperatures are given in degrees Celsius (ºC), and operations were carried out at room or ambient temperature, that is, at a temperature in the range of 18-30 ºC. In general, the course of reactions was followed by thin layer chromatography or mass spectroscopy and reaction times are given for illustration only; where a synthesis is described as being analogous to that described in a previous example, the amounts used are the millimolar ratio equivalents to those used in the previous example. NMR data is in the form of delta values for major diagnostic protons, given in parts per million (ppm) relative to tetramethylsilane (TMS) as an internal standard, determined at 300 MHz or 400 MHz using deuterated solvent. Analytical mass spectra were run with an electron energy of 70 eV in the chemical ionization (CI) mode using a direct exposure probe; where indicated ionization was effected by electron impact (EI), electrospray (ESP), or atmospheric pressure chemical ionization (APCI); values for m/z are given; generally, only ions which indicate the parent mass are reported. All final compounds were purified to

≥95% purity, as assessed by analytical HPLC using an Agilent 1100 equipped with Waters columns (Atlantis T3, 2.1 × 50 mm, 3 *μ*m or Atlantis dC18, 2.1 × 50 mm, 5 *μ*m) eluted for >10 min with a gradient mixture of water and acetonitrile with either formic acid or ammonium acetate added as a modifier, monitored at wavelengths of 220, 254, and 280 nm.

All experimental activities involving animals were carried out in accordance with AstraZeneca animal welfare protocols, which are consistent with The American Chemical Society Publications rules and ethical guidelines.

2-(3-fluorophenyl)-7-[(3*S*)-piperidin-3-ylamino]thieno[2,3-*c*]pyridine-4-carboxamide (4).

To a flask containing *tert*-butyl (3*S*)-3-{[4-cyano-2-(3-fluorophenyl)thieno[2,3-*c*]pyridin-7-yl]amino}piperidine-1-carboxylate was added approximately 2.00 mL of PPA. The reaction mixture was stirred at 110 ^{o}C for 12 h. The crude reaction mixture was then diluted with 10.0 mL of water and brought to a basic pH with 6N NaOH. The mixture was then extracted with ethyl acetate (4 x 100 mL) followed by CH_2Cl_2/MeOH (1/1, 4 x 100 mL), dried over $MgSO_4$, and concentrated under reduced pressure to yield the crude product which was purified by silica gel chromatography (100% CH_2Cl_2 to 20% MeOH/CH_2Cl_2/3% NH_4OH) to afford the title compound. ^{1}H NMR (300 MHz; d_6-DMSO; δ ppm) 8.01 (s, 1H), 7.91 (s, 1H), 7.51 (s, 1H), 7.38 (m, 1H), 7.36 (m, 2H), 7.34 (br s, 1H), 6.80 (m, 1H), 4.21 (m, 1H), 3.15 (m, 2H), 2.87 (m, 2H), 1.92-1.46 (m, 4H); LCMS (ES, M+H) = 371.

2-phenyl-4-[(3S)-piperidin-3-ylamino]thieno[3,2-c]pyridine-7-carboxamide (5).

A solution of *tert*-butyl (3*S*)-3-{[7-cyano-2-(phenyl)thieno[3,2-*c*]pyridin-4-

yl]amino}piperidine-1-carboxylate (80 mg, 0.18 mmol, Supporting Information) and 12 N HCl (conc., 4 mL) was stirred for 24 hours. Water (10-20 mL) was added and the pH of the solution was adjusted to 10-11 with sat. $NaHCO_3$. The material was isolated by filtration and was washed with a small amount of cold water. The material was dried and then purified by MPLC (SiO_2; NH_4OH/MeOH/CH_2Cl_2; 2:10:88) to give the title compound (24 mg, 38%). ^{1}H NMR (300 MHz; d_6-DMSO; δ ppm) 8.58 (s, 1H), 8.27 (s, 1H), 7.98 (br s, 1H), 7.79 (d, 2H), 7.55 (dd, 2H), 7.43 (dd, 1H), 7.34 (br s, 1H), 7.25 (d, 2H), 4.22 (m, 1H), 3.21 (d, 1H), 2.91 (d, 1H), 2.48 (m, 2H), 2.05 (m, 1H), 1.76 (m, 1H), 1.55 (m, 2H). LCMS (ES, M+H) = 353.

(2*Z*)-3-cyano-3-(3-thienyl)acrylic acid (7).

To 3-thiopheneacetonitrile (**6**, 166 mmol) was added glyoxylic acid (174 mmol), methanol (332 mL) and potassium carbonate (174 mmol). The resulting mixture was heated to reflux for three hours followed by cooling to RT. The resultant solid was filtered, rinsed with methanol, and dried in a vacuum oven to afford the desired product (**7**) (26.6 g, 90% yield). LCMS (ES, M-H) = 178.

(2*Z*)-3-cyano-3-(3-thienyl)acryloyl azide (8).

To a solution of oxalyl chloride (27.3 mL, 313 mmol) in dichloromethane (57 mL) was added (2*Z*)-3-cyano-3-(3-thienyl)acrylic acid (**7**) (26.6 g, 149 mmol) in portions. The resulting solution was stirred at RT until LCMS indicated completion of the reaction. The reaction mixture was then filtered and rinsed with dichloromethane. The filtrate was collected, concentrated under reduced pressure and dried under vacuum to afford the product as a yellow solid as the acyl chloride intermediate. To a solution of sodium

azide (12.2 g, 187 mmol) in a 1:1 mixture of dioxane/water (23 mL) was added at 0 °C the intermediate in 33 mL dioxane. The reaction was stirred for 15 minutes at 0 °C, followed by warming the reaction to RT. After approximately 1.5 h, water (100 mL) was added to the reaction and the resulting solid was filtered and dried in a vacuum oven to yield the product (**8**) (15.1 g). ^{1}H NMR (300 MHz; d_6-DMSO; δ ppm) 8.24 (s, 1 H), 7.76-7.71 (m, 2 H), 7.25 (s, 1 H). LCMS (ES, M-H) = 204.

7-oxo-6,7-dihydrothieno[2,3-*c*]pyridine-4-carbonitrile (9).

To a solution of phenyl ether (224 mL) and tributylamine (53.0 mL) at 230 °C was added dropwise (2*Z*)-3-cyano-3-(3-thienyl)acryloyl azide (**8**) in approximately 10 mL of dichloromethane. The mixture was stirred at 230 °C for thirty minutes, cooled to RT, followed by the addition of 500 mLof hexane, which afforded a yellowish solid. The resultant solid was washed with hexane and dried under vacuum to yield the product (**9**) (4.61 g, 44% yield). ^{1}H NMR (300 MHz; d_6-DMSO; δ ppm) 12.4 (br s, 1 H), 8.26 (m, 2 H), 7.42 (d, 1 H).

2-bromo-7-chlorothieno[2,3-*c*]pyridine-4-carbonitrile (10).

To a solution of 7-oxo-6,7-dihydrothieno[2,3-*c*]pyridine-4-carbonitrile (2.30 g, 13.1 mmol) in 1/1 acetic acid/DMF (10 mL) was added *N*-bromosuccinimide (11.6 g, 65.3 mmol). The reaction mixture was heated to 80 °C for one. The solution was cooled to RT and diluted with 100 mL of water. The reaction was then neutralized with saturated sodium bicarbonate followed by filtration of the resulting solid, which was dried in a vacuum oven to afford 2-bromo-7-oxo-6,7-dihydrothieno[2,3-*c*]pyridine-4-carbonitrile (3.20 g, 96% yield). ^{1}H NMR (300 MHz; d_6-DMSO; δ ppm) 12.7 (br s, 1

H), 8.41 (s, 1 H), 8.32 (d, 1 H); LCMS (ES, M+H) = 256.

To 2-bromo-7-oxo-6,7-dihydrothieno[2,3-*c*]pyridine-4-carbonitrile (3.20 g, 12.5 mmol) was added 45.0 mL of phosphorous oxychloride. The reaction was heated to reflux overnight after which LCMS indicated reaction was complete. The reaction was then cooled to RT and the volatiles were removed under reduced pressure. To the resulting residue was added approximately 200 mL of water. The black solid was filtered and rinsed with copious amounts of water and dried under vacuum to yield the title compound (2.80 g, 82% yield). ^{1}H NMR (300 MHz; d_6-DMSO; δ ppm) 8.97 (s, 1H), 8.71 (s, 1H).

tert-butyl (3*S*)-3-[(2-bromo-4-cyanothieno[2,3-*c*]pyridin-7-yl)amino]piperidine-1-carboxylate (11).

To a solution of 2-bromo-7-chlorothieno[2,3-*c*]pyridine-4-carbonitrile (2.80 g, 10.2 mmol) in *N*-methylpyrrolidine (NMP, 10.0 mL) was added potassium carbonate (4.23 g, 30.6 mmol) and *tert*-butyl (3*S*)-3-aminopiperidine-1-carboxylate (4.92 g, 24.6 mmol). The reaction mixture was heated to 130 ^{o}C until LCMS indicated the reaction was complete. The reaction mixture was then cooled to RT and approximately 100 mL of water was added. The resulting solid was filtered and vacuum dried to afford the title compound. ^{1}H NMR (300 MHz; d_6-DMSO; δ ppm) 8.47 (s, 1H), 8.35 (s, 1H), 7.90 (br s, 1H), 4.14 (m, 1H), 3.38 (m, 1H), 3.24 (m, 1H), 2.93 (m, 2H), 1.94-1.73 (m, 4H), 1.37 (s, 9H); LCMS (ES, M+H) = 338.

tert-butyl (3*S*)-3-{[4-cyano-2-(3-fluorophenyl)thieno[2,3-*c*]pyridin-7-yl]amino}piperidine-1-carboxylate (Scheme 1, step h).

To *tert*-butyl (3*S*)-3-[(2-bromo-4-cyanothieno[2,3-*c*]pyridin-7-yl)amino]piperidine-1-carboxylate (**11**, 428 mgs, 0.979 mmol) was added cesium carbonate (957 mg, 2.94 mmol), 3-fluorophenyl boronic acid (206 mgs, 1.47 mmol), $Pd(PPh_3)_4$ (113 mgs, 0.0979 mmol), and dioxane/water (4 mL/2 mL). The reaction was heated to 80 ^oC for one hour whereupon the reaction was cooled to RT, filtered, and purified using silica gel chromatography (100% hexanes to 100% ethyl acetate) to afford the title compound (241 mg, 54% yield). LCMS (ES, M+H) = 453.

2-phenyl-7-[(3S)-piperidin-3-ylamino]thieno[2,3-c]pyridine-4-carboxamide (12).

Compound **12** was prepared in a similar procedure to **4** using the phenyl boronic acid. ^1H NMR (300 MHz; d_6-DMSO; δ ppm) 8.01 (s, 1H), 7.86 (s, 1H), 7.68 (m, 1H), 7.49-7.24 (m, 5H), 7.12 (br s, 1H), 4.50 (m, 1H), 3.15 (m, 2H), 2.87 (m, 2H), 2.01-1.20 (m, 4H); LCMS (ES, M + H) = 353.

2-(3-fluorophenyl)-4-[(3S)-piperidin-3-ylamino]thieno[3,2-c]pyridine-7-carboxamide (13).

Compound **13** was prepared using a similar procedure to **5**. ^1H NMR (300 MHz; d_6-DMSO; δ ppm) 8.59 (s, 1 H) 8.34 (s, 1 H) 7.98 (s, 1 H) 7.51 - 7.64 (m, 3 H), 7.37 (s, 1 H) 7.21 - 7.30 (m, 3 H) 4.22 (s, 1 H) 3.19 (d, 1 H) 2.90 (d, 1 H) 2.38 - 2.53 (m, 2 H) 2.04 (m, 1 H) 1.75 (m, 1 H) 1.54 (m, 2 H); LCMS (ES M + H) = 371.

4-[(3S)-piperidin-3-ylamino]-2-(2-thienyl)thieno[3,2-c]pyridine-7-carboxamide (14).

Compound **14** was prepared using a similar procedure to **5**. ^1H NMR (300 MHz; d_6-

DMSO; δ ppm) 9.42 (s, 1H), 8.94 (s, 1H), 8.55 (s, 1H), 8.34 (s, 2H), 7.65 (d, 1H), 7.46 (d, 1H), 7.40 (m, 1H), 7.17 (m, 1H), 4.57 (m, 1H), 3.50 (m, 1H), 3.21 (m, 1H), 2.96 (m, 2H), 2.05 (m, 2H), 1.76 (m, 2H); LCMS (M + H) = 359.

4-[(3S)-piperidin-3-ylamino]-2-(3-thienyl)thieno[3,2-c]pyridine-7-carboxamide (15).

Compound **15** was prepared using a similar procedure to **5.** ^{1}H NMR (300 MHz; d_6-DMSO; δ ppm) 9.72 (s, 1H), 9.08 (s, 1H), 8.79 (s, 1H), 8.55 (s, 1H), 8.40 (s, 1H), 7.96 (s, 1H), 7.78 (t, 1H), 7.72 (s, 1H), 7.54 (d, 1H), 4.63 (m, 1H), 3.19 (m, 2H), 3.02 (m, 2H), 2.06 (m, 2H), 1.81 (m, 2H); LCMS (M + H) = 359.

4-[(3S)-piperidin-3-ylamino]-2-(1H-pyrazol-4-yl)thieno[3,2-c]pyridine-7-carboxamide (16).

Compound **16** was prepared using a similar procedure to **5.** ^{1}H NMR (300 MHz; d_6-DMSO; δ ppm) 1.81-1.57 (m, 2H), 2.10-1.91 (m, 2H), 2.90 (m, 2H), 3.24 (m, 1H), 3.47 (m, 1H), 4.47 (m, 1H), 7.64 (m, 1H), 7.82 (m, 1H), 8.03 (m, 3H), 8.53 (m, 1H), 8.78 (m, 2H); LCMS (M + H) = 343.

2-(1-methyl-1H-pyrazol-4-yl)-4-[(3S)-piperidin-3-ylamino]thieno[3,2-c]pyridine-7-carboxamide (17).

Compound **17** was prepared using a similar procedure to **5.** ^{1}H NMR (300 MHz; d_6-DMSO; δ ppm) 9.44 (br s, 1H), 8.89 (m, 1H), 8.47 (s, 1H), 8.45-8.20 (m, 2H), 8.18 (s, 1H), 7.80 (s, 1H), 7.63 (br s, 1H), 4.54 (m, 1H), 3.89 (s, 3H), 3.47 (m, 1H), 3.20 (m, 1H), 3.10 (m, 1H), 2.99 (m, 1H), 2.05 (m, 1H), 1.97 (m, 1H), 1.78 (m, 2H); LCMS (M + H) = 459.

2-(1-benzyl-1H-pyrazol-4-yl)-4-[(3S)-piperidin-3-ylamino]thieno[3,2-c]pyridine-7-carboxamide (18).

Compound **18** was prepared using a similar procedure to **5**. ^{1}H NMR (300 MHz; d_6-DMSO; δ ppm) 9.45 (br s, 1H), 8.90 (m, 1H), 8.48 (s, 1H), 8.41-8.14 (m, 2H), 8.33 (s, 1H), 7.85 (s, 1H), 7.61 (s, 1H), 7.39-7.27 (m, 5H), 5.38 (s, 2H), 4.54 (m, 1H), 3.47 (m, 1H), 3.18 (m, 1H), 3.08 (m, 1H), 2.97 (m, 1H), 2.05 (m, 1H), 1.97 (m, 1H), 1.77 (m, 2H); LCMS (M + H) = 433.

2-(1H-imidazol-1-yl)-4-[(3S)-piperidin-3-ylamino]thieno[3,2-c]pyridine-7-carboxamide (19).

To a solution of CuI (2.7 mg, 0.014 mmol), imidazole (46 mg, 0.670 mmol), and cesium carbonate (191 mg, 0.586 mmol) under nitrogen was added *tert*-butyl (3*S*)-3-[(7-cyano-2-iodothieno[3,2-*c*]pyridin-4-yl)amino]piperidine-1-carboxylate (Supporting Information) (135 mg, 0.279 mmol), *trans*-1,2-cyclohexanediamine (4.2 µL, 0.056 mmol) and anhydrous 1,4-dioxane (1.0 mL). The reaction mixture was stirred at 110 ^{o}C for 24 hours at which point the reaction was cooled to rt and diluted with DCM. The mixture was filtered and solvents were removed under reduced pressure. The black residue was purified by preparatory HPLC (5-95% MeCN, H_2O, 0.1% TFA) to afford the intermediate tert-butyl (3S)-3-{[7-cyano-2-(1H-indazol-1-yl)thieno[3,2-c]pyridin-4-yl]amino}piperidine-1-carboxylate. The intermediate was added to a flask containing 1.00 mL of 12 N HCl. The reaction mixture was stirred at rt. Additional 12 N HCl was added over 12 h to complete the conversion to the desired product. Upon completion, the reaction mixture was cooled to 0 ^{o}C and treated with 6 N NaOH dropwise until a pH of 12 was obtained. The mixture was extracted with EtOAc in addition to

CH_2Cl_2/MeOH (1/1), organic layers were dried over magnesium sulfate, filtered and concentrated *in vacuo* to yield the product. ^{1}H NMR (300 MHz; d_6-DMSO; δ ppm) 1.82-1.70 (m, 2H), 2.03-1.94 (m, 2H), 2.97-2.92 (m, 2H), 3.24 (m, 1H), 3.38 (m, 1H), 4.24 (m, 1H), 7.27 (m, 1H), 7.43 (m, 1H), 7.66 (s, 1H), 7.89 (s, 1H), 8.06 (br s, 1H), 8.16 (s, 1H), 8.58 (s, 1H); LCMS (ES, M + H) = 343.

2-methyl-4-[(3*S*)-piperidin-3-ylamino]thieno[3,2-*c*]pyridine-7-carboxamide (20)

To a flask containing *tert*-butyl (3*S*)-3-[(7-cyano-2-methylthieno[3,2-*c*]pyridin-4-yl)amino]piperidine-1-carboxylate was added 5.00 mL of 12 N HCl. The reaction mixture was stirred at rt and monitored by LCMS. Additional 12 N HCl was added over 12 h to afford complete conversion to the desired product. Upon completion, the reaction mixture was diluted with water and concentrated under reduced pressure to yield product, which was purified by silica gel chromatography (100% CH_2Cl_2 to 20% MeOH/CH_2Cl_2/3% NH_4OH) to afford the title compound. ^{1}H NMR (300 MHz; d_6-DMSO; δ ppm) 8.42 (s, 1 H), 7.81 (br s, 1 H), 7.41 (s, 1 H), 7.14 (s, 1 H), 7.14 (br s, 1 H), 6.96 (d, 1 H), 4.11 (m, 1 H), 3.31 (s, 3 H), 3.14 (m, 2 H), 2.82 (m, 2 H), 1.94 (m, 1 H), 1.52 (m, 1 H), 1.36 (m, 2 H); LCMS (ES, M+H) = 291.

2-phenyl-4-[(3S)-piperidin-3-ylamino]-1H-indole-7-carboxamide (21).

To a solution of 4-amino-2-phenyl-1*H*-indole-7-carboxamide (**26**) (0.60 g, 2.4 mmol) and *tert*-butyl 3-oxopiperidine-1-carboxylate (0.6 g, 2.8 mmol) dissolved in AcOH (15 mL) was added Na_2SO_4. The mixture was stirred at rt for 1h and then slowly charged with sodium triacetoxyborohydride (1.5 g, 7.2 mmol). The reaction was stirred at rt for 1h. The mixture was diluted with EtOAc and water, washed with sat. $NaHCO_3$, 1N HCl, and sat. NaCl. The organic layer was dried over Na_2SO_4, filtered, and

concentrated in vacuo. The residue was purified by silica gel column to afford the intermediate *tert*-butyl 3-{[7-(aminocarbonyl)-2-phenyl-1*H*-indol-4-yl]amino}piperidine-1-carboxylate. A stirred solution of the intermediate (0.15 g, 0.35 mmol) in MeOH (10 mL) was charged with 4.0 N HCl in dioxane (10 mL). The reaction was stirred for 2h at RT and then concentrated *in vacuo* to give the hydrochloride salt. The residue was diluted with 2.0 N NH_3 in MeOH (10 mL) and concentrated in vacuo. The residue was purified by SILICA GEL COLUMN (10% MeOH/ CH_2Cl_2/1.5% NH_4OH-20% MeOH/ CH_2Cl_2/3% NH_4OH) to give the racemic product as an off-white solid (90 mg, 78%). The racemic mixture was separated by chiral Preparatory HPLC (column: Chiralpak OD, 250 X 21 mm, 10 μm) and eluded with 85% hexane and 15% 1:1 ehtanol:methanol, 0.1% diethylamine at a flow rate of 20 mL/min. The second to elude was collected and concentrated to afford the title compound (R_t: 27.9 min, 97% e.e.) to give **21**. ^{1}H NMR (300 MHz; d_6-DMSO; δ ppm) 10.87 (s, 1 H) 7.69 (d, 2 H) 7.57 (d, 1 H) 7.45 (t, 2 H) 7.28 (t, 1 H) 7.20 (s, 1 H) 6.96 (br s, 1 H) 6.15 (d, 1 H) 6.02 (d, 1 H) 3.50 (d, 1 H) 3.30 (s, 2 H) 3.05 - 3.20 (m, 2 H) 2.84 (d, 1 H) 2.34 - 2.46 (m, 1 H) 1.98 (s, 1 H) 1.60 - 1.72 (m, 1 H) 1.43 - 1.58 (m, 2 H); LCMS (ES, M+H) = 335.

Methyl 2-amino-4-nitrobenzoate (23).

To a solution of 2-amino-4-nitrobenzoic acid (25 g, 0.137 mol) in MeOH (100 mL) was bubbled HCl (g) for 15-20 min. The resulting solution was refluxed for 2 days. Upon cooling, the crystalline product was isolated by filtration and drying under high vacuum (16.9 g, 63%). ^{1}H NMR (300 MHz; d_6-DMSO; δ ppm) 7.90 (d, 1 H) 7.67 (d, 1 H) 7.25 (dd, 1 H) 7.13 (s, 2 H) 3.84 (s, 3 H).

4-Nitro-2-phenyl-1*H*-indole-7-carboxylic acid (24).

To a solution of methyl 2-amino-4-nitrobenzoate (2.2 g, 11.2 mmol) and acetophenone (2.8 g, 23.3 mmol) in DMSO (30 mL) cooled to –15 °C was added solid KOtBu (2.7 g, 24 mmol). After stirring for 20 min., the reaction was quenched with sat. NH_4Cl (200 mL) and then stirred for an additional 1h at RT. The red precipitate was filtered, washed with water, and dried under high vacuum to give the title compound (2.85 g, 90%). ^{1}H NMR (300 MHz; d_6-DMSO; δ ppm) 12.05 (s, 1 H) 7.99 (d, 1 H) 7.89 (d, 2 H) 7.65 (d, 1 H) 7.50 (t, 2 H) 7.44 (s, 1 H) 7.41 (d, 1H) 7.30 (br s, 1 H). LCMS (ES, M-H) = 281.

4-Nitro-2-phenyl-1*H*-indole-7-carboxamide (25).

To a solution of 4-nitro-2-phenyl-1*H*-indole-7-carboxylic acid (0.60 g, 2.1 mmol) in CH_2Cl_2 (20 mL) at –15 °C was added isobutyl chloroformate (0.5 mL, 3.8 mmol). After stirring for 1h, NH_3 (g) was bubbled through the reaction mixture for 10-15 min. and then stirred for an additional 1h at RT. After removing the solvent, the residue was purified by silica gel column (50-100% EtOAc/Hexanes) to give the product as a dark yellow solid (0.50 g, 85%). (300 MHz; d_6-DMSO; δ ppm) 11.72 (s, 1 H) 8.46 (s, 1 H) 8.11 (d, 1 H) 8.02 (d, 2 H) 7.92 (s, 1 H) 7.76 (d, 1 H) 7.50 - 7.57 (m, 3 H) 7.47 (d, 1 H); LCMS (ES, M+H) = 282.

2-(3-fluorophenyl)-4-[(3S)-piperidin-3-ylamino]-1H-indole-7-carboxamide (27).

Compound **27** was prepared using a similar procedure to **21**. ^{1}H NMR (300 MHz; d_6-DMSO; δ ppm) 10.98 (s, 1H), 9.19 (m, 1H), 9.08 (m, 1H), 7.63 (d, 2H), 7.56 (m, 2H), 7.50 (m, 1H), 7.34 (s, 1H), 7.13 (dt, 1H), 6.26 (d, 1H), 5.60 (br s, 2H), 4.00 (m, 1H),

3.41 (m, 1H), 3.21 (m, 1H), 2.92 (m, 1H), 2.80 (m, 1H), 2.0 (m, 1H), 1.93 (m, 1H), 1.76 (m, 1H), 1.69 (m, 1H); LCMS (ES, M + H) = 353.

2-(4-fluorophenyl)-4-[(3S)-piperidin-3-ylamino]-1H-indole-7-carboxamide (28)

Compound **28** was prepared using a similar procedure to **21.** ^{1}H NMR (300 MHz; d_6-DMSO; δ ppm) 10.89 (s, 1H), 8.92 (m, 1H), 8.73 (m, 1H), 7.75 (d, 1H), 7.74 (d, 1H), 7.60 (d, 1H), 7.30 (t, 2H), 7.15 (d, 1H), 7.04 (br s, 1H), 6.33 (br s, 1H), 6.23 (d, 1H), 3.91 (m, 1 H), 3.41 (m, 1H), 3.25 (m, 1H), 2.89 (m, 1H), 2.75 (m, 1H), 2.03 (m, 1H), 1.94 (m, 1H), 1.74 (m, 1H), 1.66 (m, 1H); LCMS (ES, M + H) = 353.

2-(4-chlorophenyl)-4-[(3S)-piperidin-3-ylamino]-1H-indole-7-carboxamide (29).

Compound **29** was prepared using a similar procedure to **21**. ^{1}H NMR (300 MHz; d_6-DMSO; δ ppm) 10.75 (s, 1H), 9.10 (m, 2H), 7.55 (d, 2H), 7.45 (d, 1H), 7.33 (d, 2H), 7.15 (d, 1H), 6.08 (d, 1H), 5.45 (br s, 3H), 3.83 (m, 1H), 3.21 (m, 1H), 3.03 (m, 1H), 2.73 (m, 1H), 2.65 (m, 1H), 1.80 (m, 2H), 1.62 (m, 1H), 1.51 (m, 1H); LCMS (ES, M + H) = 369.

2-phenyl-4-[(3*S*)-piperidin-3-ylamino]furo[3,2-*c*]pyridine-7-carboxamide (30).

Crude *tert*-butyl (3*S*)-3-[(7-cyano-2-phenylfuro[3,2-*c*]pyridin-4-yl)amino]piperidine-1-carboxylate (178 mg) (Supporting Information) was treated with 12 N HCl (5 ml) and the mixture was stirred at rt overnight. After removal of the solvent, the residue was purified by Gilson PrepLC to give the title compound as a trifluoroacetate salt. The salt was dissolved in MeOH (1 ml), and then charged with 4N HCl/Dioxane (2 ml). After stirring overnight, the white solid was filtered and dried in the air to afford the title

compound (53 mg). ^{1}H NMR (300 MHz; d_6-DMSO; δ ppm) 9.14 (br s, 1H), 8.89 (brs, 1H), 8.34 (s, 1H), 7.91 (d, 2H), 7.85 (s, 1H), 7.67 (s, 2H), 7.55 (t, 2H), 7.45 (t, 1H), 4.47 (m, 1H), 3.19 (m, 2H), 2.96 (m, 2H), 2.03 (m, 2H), 1.72 (m, 2H). LCMS (ES, M+H) = 337.

2-Phenyl-4-[(3S)-piperidin-3-yloxy]thieno[3,2-c]pyridine-7-carboxamide (31).

A solution of *tert*-butyl (3*S*)-3-[(7-cyano-2-phenylthieno[3,2-*c*]pyridin-4-yl)oxy]piperidine-1-carboxylate (1.0 g, 2.3 mmol) and 12 N HCl (conc., 15 mL) was stirred for 12 h. Water (100 mL) was added and the solution was concentrated to dryness *in vacuo*. The white solid obtained was dissolved in 100 mL of MeOH and concentrated *in vacuo* to give the product (0.86 g, 96%) after drying under high vacuum. ^{1}H NMR (300 MHz; d_6-DMSO; δ ppm) 9.56 (d , 1 H) 9.10 (s, 1 H) 8.67 (s, 1 H) 8.32 (s, 1 H) 8.28 (s, 1 H) 7.87 (d, 2 H) 7.66 (s, 1 H) 7.49 (t, 2 H) 7.40 (t, 1 H), 5.64 (s, 1 H) 3.41 (s, 2 H) 3.17 - 3.28 (m, 1 H) 3.03 (d, 1 H) 1.91 - 2.06 (m, 3 H) 1.65 - 1.79 (m, 1 H). LCMS (ES, M + H) = 354.

2-Phenyl-4-(piperidin-3-ylthio)thieno[3,2-c]pyridine-7-carboxamide (32).

Prepared using a similar procedure to **5** with benzyl 3-mercaptopiperidine-1-carboxylate (synthesis in Supporting Information) as the corresponding reagent. ^{1}H NMR (300 MHz; d_6-DMSO; δ ppm) 9.23 (br, 2H), 8.91 (s, 1H), 8.45 (s, 1H), 7.88 (d, 2H), 7.83 (br, 1H), 7.82 (s, 1H), 7.50 (t, 2H), 7.43 (t, 1H), 4.41 (m, 1H), 3.63 (m, 1H), 3.23 (m, 1H), 3.09 (m, 1H), 2.94 (m, 1H), 2.22-2.13 (m, 1H), 1.96-1.72 (m, 3H); LCMS (ES, M+H) = 370.

4-{methyl[(3S)-piperidin-3-yl]amino}-2-phenylthieno[3,2-c]pyridine-7-carboxamide (33).

Compound 33 was prepared using a similar procedure to 5 but using *tert*-butyl (3*S*)-3-(methylamino)piperidine-1-carboxylate (synthesis in Supporting Information) as the starting material. ^{1}H NMR (300 MHz; d_6-DMSO; δ ppm) 9.26 (br s, 1H), 8.92 (br s, 1H), 8.59 (s, 1H), 8.18 (br s, 1H), 7.94 (s, 1H), 7.85 (m, 2H), 7.46 (m, 2H), 7.40 (m, 1H), 4.83 (m, 1H), 3.42 (m, 1H), 3.29 (s, 3H), 3.22 (m, 2H), 2.89 (m, 1H), 2.00-1.79 (m, 4H). LCMS (ES, M + H) = 367.

4-{ethyl[(3S)-piperidin-3-yl]amino}-2-phenylthieno[3,2-c]pyridine-7-carboxamide (34).

Compound **34** was prepared using a similar procedure to **5** but using *tert*-butyl (3*S*)-3-(ethylamino)piperidine-1-carboxylate as the corresponding reagent. ^{1}H NMR (300 MHz; d_6-DMSO; δ ppm) 9.26(b, 1H), 8.95(b, 1H), 8.63(s, 1H), 8.19 (b, 1H),7.86 (m, 2H), 8.77(s, 1H), 7.49(m, 3H), 7.40(m,2H), 4.75(m, 1H), 3.77 (m, 2H), 3.40(m, 1H), 3.23(m, 2H), 2.87(m, 1H), 1.96(m, 3H), 1.74(m, 1H), 1.17(t, 3H); LCMS (ES, M + H) = 381.

4-{(2-hydroxyethyl)[(3S)-piperidin-3-yl]amino}-2-phenylthieno[3,2-c]pyridine-7-carboxamide (35).

Compound **35** was prepared using a similar procedure to **5** but using (*S*)-*tert*-butyl 3-(2-hydroxyethylamino)piperidine-1-carboxylate as the corresponding reagent. ^{1}H NMR (300 MHz; d_6-DMSO + D_2O; δ ppm) 8.57 (s, 1H), 7.80 (s, 1H), 7.77 (m, 2H), 7.49 (m, 2H), 7.39 (m, 1H), 4.59 (m, 1H), 3.77 (m, 1H), 3.69 (m, 1H), 3.54 (m, 2H), 3.39 (m, 1H), 3.20 (m, 2H), 2.82 (m, 1H), 1.89 (m, 3H), 1.70 (m, 1H); LCMS (ES, M +

H) = 397.

2-phenyl-4-{(2-phenylethyl)[(3S)-piperidin-3-yl]amino}thieno[3,2-c]pyridine-7-carboxamide (36).

Compound **36** was prepared using a similar procedure to **5** but using (*S*)-tert-butyl 3-(phenethylamino)piperidine-1-carboxylate as the corresponding reagent. ^{1}H NMR (300 MHz; d_6-DMSO + D_2O; δ ppm) 8.63 (s, 1H), 767 (m, 2H), 7.53 (s, 1H), 7.44 (m, 3H), 7.14-7.23 (m, 5H), 4.50 (m, 1H), 3.85 (m, 2H), 3.15 (m, 3H), 2.80 (m, 3H), 1.80-1.87 (m, 3H), 1.66 (m, 1H); LCMS (ES, M + H) = 457.

***tert*-butyl ((1*S*)-1-acetyl-4-{[(benzyloxy)carbonyl]amino}butyl)carbamate (38).**

To a 3-necked flask containing N^5-[(benzyloxy)carbonyl]-N^2-(*tert*-butoxycarbonyl)-L-ornithine (**37**) (36.6 g, 100 mmol) equipped with a magnetic stir bar and an addition funnel was added dry THF (100 mL). The addition funnel was charged with MeLi (1.6 M in ether; 275 mL; 440 mmol), which was subsequently added slowly (over 20 minutes) to the reaction mixture cooled to 0^{o}C. This solution was then warmed to rt. After stirring for an additional 5 h, the reaction was quenched by pouring onto a stirred ice/water mixture. The aqueous mixture was extracted with EtOAc (3 x 100 mL). The combined organic layers were then washed with brine, dried over Na_2SO_4, filtered and concentrated *in vacuo* to yield a yellow oil (6.0 g, 98%). After purification using MPLC (SiO_2; 25-60% EtOAc/hexanes), the product was isolated as a clear oil (5.2 g, 14%). ^{1}H NMR (300 MHz; d_6-DMSO; δ ppm) 7.35 (m, 5H), 7.25 (m, 2H), 5.00 (s, 2H), 3.85 (m, 1H), 2.98 (dd, 2H), 2.05 (s, 3H), 1.63 (m, 1H), 1.39 (s, 9H), 1.34 (m, 3H). LCMS (ES, M+H) = 365.

tert-butyl-2-methylpiperidin-3-ylcarbamate (39).

To a stirred solution of *tert*-butyl ((1*S*)-1-acetyl-4-{[(benzyloxy)carbonyl]amino}butyl)carbamate (**38**) (3.9 g, 10.7 mmol) in MeOH (200 mL) was added 10% Pd/C (0.1 mmol). The heterogeneous mixture was hydrogenated at atmospheric pressure for 3 days (or 40 psi overnight). The product as the mixture of four diastereomers was isolated as clear oil after filtration through diatomaceous earth and evaporation of the filtrate to give the product without further purification (2.3 g; 100%). LCMS (ES, M+H) = 215.

(trans)-benzyl 3-(tert-butoxycarbonylamino)-2-methylpiperidine-1-carboxylate (40).

To a stirred solution of *tert*-butyl [trans-2-methylpiperidin-3-yl]carbamate (**39**) (2.3 g, 10.7 mmol) and diisopropylethylamine (2.1 mL, 12 mmol) dissolved in CH_2Cl_2 (40 mL) cooled to 0^{o}C was added benzyl chloroformate (1.7 mL, 12 mmol). The reaction mixture was then warmed to rt and stirred for an additional 1 h. The mixture was then diluted with CH_2Cl_2 and washed with 1N HCl and brine, dried over Na_2SO_4, filtered and concentrated *in vacuo* to yield a yellow oil. After purification using MPLC (SiO_2; 10-40% EtOAc/Hexanes), the product (trans diastereomer) was isolated as a crystalline solid (1.8 g, 49% yield). ^{1}H NMR (300 MHz; d_6-DMSO; δ ppm) 7.34 (m, 5H), 6.99 (d, 1H), 5.04 (s, 2H), 4.28 (dd, 1H), 3.83 (m, 1H), 3.37 (m, 1H), 2.86 (m, 1H), 1.77 (m, 2H), 1.46 (m, 1H), 1.36 (s, 9H), 1.33 (m, 1H), 1.11 (d, 3H). LCMS (ES, M+H=349). The cis diastereomer, (*cis*)-benzyl 3-(tert-butoxycarbonylamino)-2-methylpiperidine-1-carboxylate was also isolated pure (1.3 g, 35% yield). ^{1}H NMR (300 MHz; d_6-DMSO; δ ppm) 7.35 (m, 5H), 6.97 (d, 1H), 5.07 (s, 2H), 4.44 (m, 1H),

3.80 (m, 1H), 3.40 (m, 1H), 2.78 (m, 1H), 1.63 (m, 1H), 1.49 (m, 2H), 1.39 (s, 9H), 1.36 (m, 1H), 0.96 (d, 3H). LCMS (ES, M+H) = 349.

(*trans*)-benzyl 3-amino-2-methylpiperidine-1-carboxylate (41).

To a solution of benzyl *trans*-3-[(*tert*-butoxycarbonyl)amino]-2-methylpiperidine-1-carboxylate (1.8 g, 5.2 mmol) dissolved in MeOH (10 mL) was added HCl (4 N in dioxane; 20 mL). After stirring for 1 hour at rt, the reaction was concentrated *in vacuo*, redissolved in MeOH, and then concentrated *in vacuo* to yield the hydrochloride salt of the title compound as a clear crystalline solid (1.46 g, 100%). ^{1}H NMR (300 MHz; d_6-DMSO; δ ppm) 8.27 (br s, 3H), 7.39 (m, 3H), 7.35 (m, 1H), 7.32 (m, 1H), 5.09 (s, 2H), 4.36 (dd, 1H), 3.88 (m, 1H), 3.26 (m, 1H), 2.92 (m, 1H), 1.79 (m, 3H), 1.48 (m, 1H), 1.16 (d, 3H). LCMS (ES, M+H) = 249.

(*cis*)-benzyl 3-amino-2-methylpiperidine-1-carboxylate (42).

To a solution of benzyl cis-3-[(*tert*-butoxycarbonyl)amino]-2-methylpiperidine-1-carboxylate (1.2 g, 3.4 mmol) dissolved in MeOH (10 mL) was added HCl (4N in dioxane; 20 mL). After stirring for 1h at rt, the reaction was concentrated *in vacuo*, redissolved in MeOH, and then concentrated *in vacuo* to yield the hydrochloride salt of the title compound as a clear crystalline solid (0.97 g, 100%). ^{1}H NMR (300 MHz; d_6-DMSO; δ ppm) 8.39 (br s, 3H), 7.36 (m, 3H), 7.33 (m, 2H), 5.09 (s, 2H), 4.61 (dd, 1H), 3.83 (m, 1H), 3.26 (m, 1H), 2.86 (m, 1H), 1.72 (m, 3H), 1.41 (m, 1H), 1.10 (d, 3H). LCMS (ES, M+H) = 249.

4-((2*R*,3*S*)-2-methylpiperidin-3-ylamino)-2-phenylthieno[3,2-c]pyridine-7-carboxamide (44)

Prepared in a similar route to compound **5** but using benzyl *trans*-3-amino-2-methylpiperidine-1-carboxylate (**41**) as the starting material (**Scheme 1**, step g), followed by chiral preparatory HPLC separation (column: Chiralcel OD, 250 X 20 mm, 10 μm) and eluded with 85% hexane and 15% 1:1 ehtanol:methanol, 0.1% diethylamine at a flow rate of 20 mL/min. The second to elude was collected and concentrated to afford the title compound (R_t: 14.2 min, 98.7% e.e.). ^{1}H NMR (300 MHz; d_6-DMSO; δ ppm) 9.47 (m, 1 H), 9.04 (m, 1 H), 8.59 (m, 1 H), 8.45 (s, 1 H), 8.25 (m, 1 H), 7.71 (d, 2 H), 7.56 (m, 1 H), 7.45 (m, 2 H), 7.35 (m, 1 H), 4.34 (m, 1 H), 3.42 (m, 1 H), 3.22 (m, 1 H), 2.82 (m, 1 H), 2.07 (m, 1 H), 1.83 (m, 2 H), 1.59 (m, 1 H), 1.26 (d, 3 H). LCMS (ES, M+H) = 367.

4-((2*S*,3*S*)-2-methylpiperidin-3-ylamino)-2-phenylthieno[3,2-c]pyridine-7-carboxamide (45)

Prepared in a similar route to compound **44** but using benzyl (*cis*)-benzyl 3-amino-2-methylpiperidine-1-carboxylate as the starting material in step g, **Scheme** 1, followed by chiral preparatory HPLC separation (column: Chiralpak OD, 250 X 21 mm, 10 μm) and eluded with 85% hexane and 15% 1:1 ethanol:methanol, 0.1% diethylamine at a flow rate of 20 mL/min. The second to elude was collected and concentrated to afford the title compound (R_t: 12.3 min, 98% e.e.). ^{1}H NMR (300 MHz; d_6-DMSO; δ ppm) 9.79 (m, 1H), 8.95 (m, 2H, 8.51 (s, 1H), 8.15 (m, 1H), 7.78 (d, 2H), 7.49 (m, 3H), 7.38 (m, 1H), 4.73 (m, 1H), 3.71 (m, 1H), 3.28 (m, 1H), 3.00 (m, 1H), 1.95 (m, 2H), 1.82 (m, 1H), 1.69 (m, 1H), 1.30 (d, 3H); LCMS (ES, M+H) = 367.

Trans-4-[(4-hydroxypiperidin-3-yl)amino]-2-phenylthieno[3,2-c]pyridine-7-

carboxamide (46).

Prepared in a similar route to compound **5** but using benzyl trans-3-amino-4-hydroxypiperidine-1-carboxylate[14] as the starting material in step g, **Scheme 1**. ^{1}H NMR (300 MHz; d_6-DMSO; δ ppm) 9.29 (m, 1H), 8.85 (m, 1H), 8.60 (m, 1H), 8.51 (s, 1H), 8.19 (m, 1H), 7.77 (d, 2H), 7.56 (m, 1H), 7.50 (dd, 2H), 7.40 (dd, 1H), 4.42 (m, 1H), 4.0-4.3 (br s, 1H), 3.88 (m, 1H), 3.51 (m, 1H), 3.27 (m, 1H), 3.05 (m, 2H), 2.16 (m, 1H), 1.73 (m, 1H); LCMS (ES, M+H) = 369.

4-{[trans-2-(2-hydroxyethyl)piperidin-3-yl]amino}-2-phenylthieno[3,2-c]pyridine-7-carboxamide (47).

Prepared in a similar route to compound **5** but using benzyl trans-3-amino-2-(2-hydroxyethyl)piperidine-1-carboxylate (synthesis in Supporting Information) as the starting material in step g, **Scheme 1**. ^{1}H NMR (300 MHz; d_6-DMSO; δ ppm) 9.57 (m, 1H), 8.92 (m, 1H), 8.61 (s, 1H), 8.14 (br s, 1H), 7.97 (s, 1H), 7.87 (d, 2H), 7.50 (m, 3H), 7.40 (m, 1H), 4.82 (m, 1H), 3.55 (m, 1H), 3.29 (s, 3H), 3.23 (m, 1H), 2.94 (m, 1H), 1.97 (m, 4H), 1.21 (d, 3H). LCMS (ES, M + H) = 381.

4-[(*cis*-2,6-dimethylpiperidin-3-yl)amino]-2-phenylthieno[3,2-*c*]pyridine-7-carboxamide (48).

To a flask containing 4-[(*cis*-2,6-dimethylpiperidin-3-yl)amino]-2-phenylthieno[3,2-*c*]pyridine-7-carbonitrile was added 5.00 mL of 12 N HCl. The reaction mixture was stirred at rt. Additional 12 N HCl was added over 12 h to afford complete conversion to the desired product. Upon completion, the reaction mixture was diluted with MeOH and concentrated under reduced pressure to yield the product, which was purified by preparatory HPLC (5%-95% H_2O/MeCN/0.1% TFA) to afford the title

compound as a mixture of isomers. Analytical data provided for major isomer present in mixture: ^{1}H NMR (300 MHz; d_6-DMSO; δ ppm) 9.96 (m, 1H), 9.19 (m, 1H), 9.02 (m, 1H), 8.50 (s, 1H), 8.21 (m, 1H), 7.79 (m, 2H), 7.49 (m, 2H), 7.35 (m, 2H), 4.74 (m, 1H), 3.67 (m, 1H), 3.27 (m, 1H), 1.84 (m, 4H), 1.36 (m, 6H). LCMS (ES, M+H) = 381.

4-(*cis*-6-methylpiperidin-3-ylamino)-2-phenylthieno[3,2-c]pyridine-7-carboxamide (49).

Prepared in a similar route to compound **48** but using benzyl *trans*-2-methyl-5-(methylamino)piperidine-1-carboxylate (synthesized similarly to **48**, Supporting Information) as the starting material in step g, **Scheme 1**. ^{1}H NMR (300 MHz; d_6-DMSO; δ ppm) 9.84 (m, 1H), 9.41 (m, 1H), 9.18 (m, 1H), 8.53 (s, 1H), 8.40 (m, 1H), 7.72 (m, 3H), 7.51 (m, 3H), 4.72 (m, 1H), 3.21 (m, 3H), 1.89 (m, 4H), 1.34 (m, 3H); LCMS (ES, M +H) = 367.

AUTHOR INFORMATION

Corresponding Author

*Phone: +1 781-839-4135. E-mail: bin.yang@astrazeneca.com

Present Addresses

$^{\perp}$Department of Biochemistry and Molecular Biophysics, Washington University School of Medicine, 660 S. Euclid Avenue, Box 8231, St. Louis, MO 63110, United States.

[∞]Mersana Therapeutics Inc., 830 Memorial Drive, Cambrige, MD 02139, United States.

[×]AstraZeneca-Innovation Center China (ICC), 898 Halei Road, Zhangjiang Hi-Tech Park, Pudong New Area 201203, China.

[¶]Theravance BioPharma, 901 Gateway Boulevard, South San Francisco, CA 94080

NOTES

The authors declare no competing financial interest.

ABBREVIATIONS USED

APCI, atmospheric pressure chemical ionization; ATP, adenosine 5-triphosphate; $CDCl_3$, deuterated hloroform; CI, chemical ionization; EI, electron impact; ESP, electrospray; iv, intravenous; LCMS, liquid chromatography-mass spectrometry; TCU, thiophenecarboxamide urea; 4-CTP, thieno[2,3-c]pyridine-4-carboxamide; 7-CTP, thieno[3,2-c]pyridine-7-carboxamide; DMSO, dimethylsulfoxide; PK, pharmacokinetics; PD, pharmacodynomics; EtOAc, ethyl acetate; DCM, dichloromethane; THF, tetrahydrofuran; MgSO4, magnesium sulfate; Boc, *tert*-Butyloxycarbonyl; Cbz, tert-Butyloxycarbonyl.

ASSOCIATED CONTENT

Supporting Information

The Supporting Information is available free of charge on the ACS Publications website at XXXXX. Complete experimental for the syntheses of compounds **5**, **19**,

20, **31**, **32**, **33**, **43**, **47**, and **48**; assays protocols on solubility, logD, and rat microsome clint, and hERG inhibition; experimental details on crystallographic information.

PDB ID Codes:

13: 6FC8; **21**: 6FCK; **44**: 6FCF.

Authors will release the atomic coordinates and experimental data upon article publication.

References

(1) Helleday, T.; Petermann, E.; Lundin, C.; Hodgson, B.; Sharma, R. A. DNA repair pathways as targets for cancer therapy. *Nat. Re. Cancer.* **2008**, *8*, 193-204.

(2) Kastan, M. B.; Bartek, J. Cell-cycle checkpoints and cancer. *Nature* **2004**, *432*, 316-323.

(3) Bunch, R. T.; Eastman, A. Enhancement of cisplatin-induced cytotoxicity by 7-hydroxystaurosporine (UCN-01), a new G2-checkpoint inhibitor. *Clin. Can. Res.* **1996**, *2*, 791.

(4) Bucher, N.; Britten, C. D. G2 checkpoint abrogation and checkpoint kinase-1 targeting in the treatment of cancer. *Br. J. Cancer* **2008**, *98*, 523-528.

(5) Ma, C. X.; Janetka, J. W.; Piwnica-Worms, H. Death by releasing the breaks: CHK1 inhibitors as cancer therapeutics. *Trends Mol. Med.* **2011**, *17*, 88-96.

(6) Reader, J. C.; Matthews, T. P.; Klair, S.; Cheung, K. M.; Scanlon, J.; Proisy, N.; Addison, G.; Ellard, J.; Piton, N.; Taylor, S.; Cherry, M.; Fisher, M.; Boxall, K.; Burns, S.; Walton, M. I.; Westwood, I. M.; Hayes, A.; Eve, P.; Valenti, M.; de Haven Brandon, A.; Box, G.; van Montfort, R. L.; Williams, D. H.; Aherne, G. W.; Raynaud, F. I.; Eccles, S. A.; Garrett, M. D.;

Collins, I. Structure-guided evolution of potent and selective CHK1 inhibitors through scaffold morphing. *J. Med. Chem.* **2011**, *54*, 8328-8342.

(7) Lainchbury, M.; Matthews, T. P.; McHardy, T.; Boxall, K. J.; Walton, M. I.; Eve, P. D.; Hayes, A.; Valenti, M. R.; de Haven Brandon, A. K.; Box, G.; Aherne, G. W.; Reader, J. C.; Raynaud, F. I.; Eccles, S. A.; Garrett, M. D.; Collins, I. Discovery of 3-alkoxyamino-5-(pyridin-2-ylamino)pyrazine-2-carbonitriles as selective, orally bioavailable CHK1 inhibitors. *J. Med. Chem.* **2012**, *55*, 10229-10240.

(8) Dudkin, V. Y.; Rickert, K.; Kreatsoulas, C.; Wang, C.; Arrington, K. L.; Fraley, M. E.; Hartman, G. D.; Yan, Y.; Ikuta, M.; Stirdivant, S. M.; Drakas, R. A.; Walsh, E. S.; Hamilton, K.; Buser, C. A.; Lobell, R. B.; Sepp-Lorenzino, L. Pyridyl aminothiazoles as potent inhibitors of Chk1 with slow dissociation rates. *Bioorg. Med. Chem. Lett.* **2012**, *22*, 2609-2612.

(9) Dudkin, V. Y.; Wang, C.; Arrington, K. L.; Fraley, M. E.; Hartman, G. D.; Stirdivant, S. M.; Drakas, R. A.; Rickert, K.; Walsh, E. S.; Hamilton, K.; Buser, C. A.; Hardwick, J.; Tao, W.; Beck, S. C.; Mao, X.; Lobell, R. B.; Sepp-Lorenzino, L. Pyridyl aminothiazoles as potent Chk1 inhibitors: optimization of cellular activity. *Bioorg. Med. Chem. Lett.* **2012**, *22*, 2613-2619.

(10) Huang, X.; Cheng, C. C.; Fischmann, T. O.; Duca, J. S.; Yang, X.; Richards, M.; Shipps, G. W., Jr. Discovery of a novel series of CHK1 kinase inhibitors with a distinctive hinge binding mode. *ACS Med. Chem. Lett.* **2012**, *3*, 123-128.

(11) Song, P.; Peng, P.; Han, M.; Cao, X.; Ma, X.; Liu, T.; Zhou, Y.; Hu, Y. Design, synthesis and biological evaluation of thienopyridinones as Chk1 inhibitors. *Bioorg. Med. Chem.* **2014**, *22*, 4882-4892.

(12) Gazzard, L.; Appleton, B.; Chapman, K.; Chen, H.; Clark, K.; Drobnick, J.; Goodacre, S.; Halladay, J.; Lyssikatos, J.; Schmidt, S.; Sideris, S.; Wiesmann, C.; Williams, K.; Wu, P.; Yen, I.; Malek, S. Discovery of the 1,7-diazacarbazole class of inhibitors of checkpoint kinase 1. *Bioorg. Med. Chem. Lett.* **2014**, *24*, 5704-5709.

(13) Janetka, J. W.; Almeida, L.; Ashwell, S.; Brassil, P. J.; Daly, K.; Deng, C.; Gero, T.; Glynn, R. E.; Horn, C. L.; Ioannidis, S.; Lyne, P.; Newcombe, N. J.; Oza, V. B.; Pass, M.;

Springer, S. K.; Su, M.; Toader, D.; Vasbinder, M. M.; Yu, D.; Yu, Y.; Zabludoff, S. D. Discovery of a novel class of 2-ureido thiophene carboxamide checkpoint kinase inhibitors. *Bioorg. Med. Chem. Lett.* **2008**, *18*, 4242-4248.

(14) Oza, V.; Ashwell, S.; Almeida, L.; Brassil, P.; Breed, J.; Deng, C.; Gero, T.; Grondine, M.; Horn, C.; Ioannidis, S.; Liu, D.; Lyne, P.; Newcombe, N.; Pass, M.; Read, J.; Ready, S.; Rowsell, S.; Su, M.; Toader, D.; Vasbinder, M.; Yu, D.; Yu, Y.; Xue, Y.; Zabludoff, S.; Janetka, J. Discovery of checkpoint kinase inhibitor (S)-5-(3-fluorophenyl)-N-(piperidin-3-yl)-3-ureidothiophene-2-carboxamide (AZD7762) by structure-based design and optimization of thiophenecarboxamide ureas. *J. Med. Chem.* **2012**, *55*, 5130-5142.

(15) Oza, V.; Ashwell, S.; Brassil, P.; Breed, J.; Deng, C.; Ezhuthachan, J.; Haye, H.; Horn, C.; Janetka, J.; Lyne, P.; Newcombe, N.; Otterbien, L.; Pass, M.; Read, J.; Roswell, S.; Su, M.; Toader, D.; Yu, D.; Yu, Y.; Valentine, A.; Webborn, P.; White, A.; Zabludoff, S.; Zheng,

X. Discovery of a novel class of triazolones as checkpoint kinase inhibitors--hit to lead exploration. *Bioorg. Med. Chem. Lett.* **2010**, *20*, 5133-5138.

(16) Daly, K.; Heron, N.; Hird, A.; Ioannidis, S.; Janetka, J., Walter; Lyne, P.; Scott, J.; Toader, D.; Vasbinder, M.; Yu, D.; Yu, Y Substituted Heterocycles and their Use as CHK1, PDK1 and PAK Inhibitors. WO2006106326 A1, October 12, 2006.

(17) Beno, B. R.; Yeung, K. S.; Bartberger, M. D.; Pennington, L. D.; Meanwell, N. A. A Survey of the role of noncovalent sulfur interactions in drug design. *J. Med. Chem.* **2015**, *58*, 4383-4438.

(18) Zhao, L.; Zhang, Y.; Dai, C.; Guzi, T.; Wiswell, D.; Seghezzi, W.; Parry, D.; Fischmann, T.; Siddiqui, M. A. Design, synthesis and SAR of thienopyridines as potent CHK1 inhibitors. *Bioorg. Med. Chem. Lett.* **2010**, *20*, 7216-7221.

(19) Cashman, J. R.; Zhang, J. Human flavin-containing monooxygenases. *Annu. Rev. Pharmacol. Toxicol.* **2006**, *46*, 65-100.

(20) Smith, D. A.; Beaumont, K.; Maurer, T. S.; Di, L. Volume of distribution in drug design. *J. Med. Chem.* **2015**, *58*, 5691-5698.

(21) Zabludoff, S. D.; Deng, C.; Grondine, M. R.; Sheehy, A. M.; Ashwell, S.; Caleb, B. L.; Green, S.; Haye, H. R.; Horn, C. L.; Janetka, J. W.; Liu, D.; Mouchet, E.; Ready, S.; Rosenthal, J. L.; Queva, C.; Schwartz, G. K.; Taylor, K. J.; Tse, A. N.; Walker, G. E.; White, A. M. AZD7762, a novel checkpoint kinase inhibitor, drives checkpoint abrogation and potentiates DNA-targeted therapies. *Mol. Can. Ther.* **2008**, *7*, 2955-2966.

(22) Seto, T.; Esaki, T.; Hirai, F.; Arita, S.; Nosaki, K.; Makiyama, A.; Kometani, T.; Fujimoto, C.; Hamatake, M.; Takeoka, H.; Agbo, F.; Shi, X. Phase I, dose-escalation study of AZD7762 alone and in combination with gemcitabine in Japanese patients with advanced solid tumours. *Cancer Chemother. Pharmacol.* **2013**, *72*, 619-627.

(23) Sausville, E.; Lorusso, P.; Carducci, M.; Carter, J.; Quinn, M. F.; Malburg, L.; Azad, N.; Cosgrove, D.; Knight, R.; Barker, P.; Zabludoff, S.; Agbo, F.; Oakes, P.; Senderowicz, A. Phase I dose-escalation study of AZD7762, a checkpoint kinase inhibitor, in combination

with gemcitabine in US patients with advanced solid tumors. *Cancer Chemther. Pharmacol.* **2014**, *73*, 539-549.

Table of Contents graphic